From electron depletion to quasi-neutrality: the sheath–bulk transition in RF modulated discharges

2009 J. Phys. D: Appl. Phys. 42 194009

(http://iopscience.iop.org/0022-3727/42/19/194009)

J. Phys. D: Appl. Phys. **42** (2009) 194009 (16pp) doi:10.1088/0022-3727/42/19/194009

From electron depletion to quasi-neutrality: the sheath–bulk transition in RF modulated discharges

Ralf Peter Brinkmann

Institute for Theoretical Electrical Engineering, Ruhr University Bochum, D-44780 Bochum, Germany

Received 12 May 2009, in final form 3 July 2009
Published 18 September 2009
Online at stacks.iop.org/JPhysD/42/194009

Abstract

The boundary sheaths of all plasmas are characterized by a gradual transition from unipolarity (electron depletion, $n_e \ll n_i$) to ambipolarity (quasi-neutrality, $n_e \approx n_i$). Capacitively driven sheaths exhibit a transition which is expanded by the RF modulation and smoothed by thermal effects, i.e. by the finiteness of the electron temperature T_e and the Debye length $\lambda_D = \sqrt{\epsilon_0 T_e/e^2 n_e}$. Sheath models which neglect thermal effects ('step models') are restricted to strongly modulated high voltage sheaths with $V_{RF} \gg T_e/e$ and fail when this condition is not met. This work presents an improved analysis of the sheath–bulk transition which takes both modulation and thermal effects into account. Based on a previously found asymptotic solution of the Boltzmann–Poisson equation (Brinkmann 2007 *J. Appl. Phys.* **102** 093393), approximate algebraic (i.e. closed) expressions for the phase-resolved electrical field E and electron density n_e in RF sheaths are derived. Under the assumption that the modulation is periodic (not necessarily harmonic) with $\omega_{RF} \gg \omega_{pi}$, also the phase averages of the field $\bar{E}$ and the electron density $\bar{n}_e$ can be expressed in closed form. These results—together referred to as the advanced algebraic approximation (AAA)—make it possible to formulate efficient and accurate models for RF driven boundary sheaths for all ratios of V_{RF} to T_e/e. As an example, a harmonically RF modulated, collision-dominated single species sheath is studied. The outcome is compared both with the numerically constructed exact solution and with the well-known step model approach of Lieberman (1989 *IEEE Trans. Plasma Sci.* **17** 338). It is found that the AAA can reproduce the exact numerical solution within a few per cent for all ratios of V_{RF} to T_e/e. The step model, in contrast, exhibits strong deviations even for large eV_{RF}/T_e and fails completely in the case of weak modulation.

1. Introduction

Electrons are light, ions are heavy. The mass ratio m_i/m_e equals at least 1836 (for hydrogen) but lies more often around 10^5 (e.g. 7.3×10^4 for argon). Also the mean energy of the two species is very different, the ratio of the temperatures T_e and T_i is typically 10^2. Electrons are therefore much more mobile than ions, the ratio of the thermal velocities is $v_{the}/v_{thi} \approx 3 \times 10^3$. For a bounded plasma, this fundamental fact implies the presence of a non-neutral (electron depleted) plasma boundary sheath in front of all material surfaces: steady state can only be maintained if a potential V_{sh} exists which confines the electrons to the quasi-neutral bulk and reduces their wall loss to the level of the ions. The thickness s of the sheath scales with $\sqrt{\epsilon_0 V_{sh}/en_i}$, where n_i is an average ion density. In capacitive plasmas, the sheath is modulated and the extension $s(t)$ of the depletion zone varies between $s_{min} \approx 0$ at the 'sheath collapse' and s_{max} during the sheath maximum. Both s_{max} and the mean sheath extension $\bar{s}$ scale with $\sqrt{\epsilon_0 V_{RF}/en_i}$. It is important to note that the actual transition from electron depletion to quasi-neutrality takes place in a much narrower zone which has a thickness of a few Debye lengths $\lambda_D = \sqrt{\epsilon_0 T_e/e^2 n_i}$. In a typical RF plasma, $eV_{RF}/T_e \approx 100$ and thus $\lambda_D/\bar{s} \ll 1$. (The notion of a 'one-dimensional' geometry, implicit in this discussion, can be justified for most cases of practical interest. The discharge may be inherently planar, such as many industrial process plasmas, or the sheath thickness much smaller than the other length

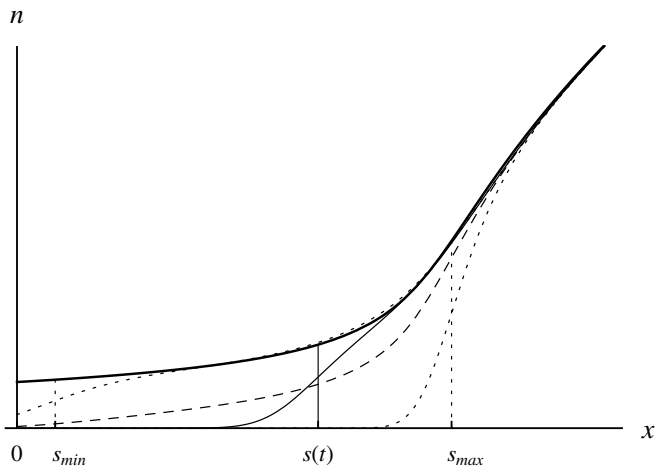

Figure 1. Schematic sketch of the particle densities in an RF driven sheath. The x-axis points from the electrode $x_E = 0$ into the bulk (note that several other conventions are used in the literature). Shown are the stationary ion density $n_i(x)$ (solid) and the momentaneous electron density $n_e(x, t)$ at a certain RF phase t (thin). The average electron density $\bar{n}_e(x)$ is dashed. Also shown are the momentaneous location $s(t)$ of the equivalent electron edge, and the minimal and maximal values of that quantity, s_{min} and s_{max}. Note that the value of s_{min} is generally different from the position of the electrode, and that s_{max} is only an approximate indicator of the sheath edge.

scales involved. Figure 1 defines the employed coordinates and other conventions. Note that several other conventions are used in the literature.)

The analysis of the RF sheath dynamics is quite complicated, even under the simplifying assumption of $\omega_{pi} \ll \omega_{RF} \ll \omega_{pe}$. (In this 'radio-frequent' regime, the existence of which is also a consequence of the large mass ratio m_i/m_e, the electrons are in equilibrium with the time-varying field, while the ions react only on its phase average and are not modulated.) Assume, for the moment, that the spatially resolved ion density $n_i(x)$ and the phase-resolved sheath charge $Q(t)$ are known. The self-consistent calculation of the electrical field $E(x, t)$ from Poisson's equation and the electron equilibrium condition amounts to solving a nonlinear differential equation. The mean field can then be found by averaging over the phase. $\bar{E}(x)$, in turn, enters the calculation of the ion density $n_i(x)$ via the ion equation of motion. Together, the relations constitute a system of nonlinear integro-differential equations for which no analytical solutions exist.

Of course, one may approach the equations numerically, or resort to direct simulation techniques like particle-in-cell (PIC). Those methods, however, are computationally costly, and do not deliver the same physical insight as analytical or semi-analytical descriptions. Many attempts have therefore been made to reduce the mathematical complexity of the problem by introducing so-called 'assumptions', i.e. simplifications which bypass certain mathematical difficulties. This work concerns itself with a very popular such assumption, the so-called 'step model', which was introduced by Godyak and Ghanna in 1979 and has found use in many subsequent studies [1–19] (not an exhaustive list).

The step model is based on the above-mentioned insight that the transition in a sheath from electron depletion to quasi-neutrality is relatively abrupt, and takes it to its extreme. It replaces the steep but smooth transition by a literal step, i.e. assumes that the electron density $n_e(x, t)$ is zero below the electron edge $s(t)$ and equal to the ion density $n_i(x)$ above. This is equivalent to neglecting thermal effects, i.e. to taking $\lambda_D \to 0$ or $T_e \to 0$.

The mathematical simplifications gained by the step assumption are quite considerable. Poisson's equation can be integrated directly, yielding a closed, algebraic representation of the electrical field in terms of $\int n_i \, dx$. (Here and throughout the paper, the term 'algebraic' is used in its wider sense, i.e. as 'not requiring the solution of a differential equation'.) By considering the phase average of that expression together with the ion equation of motion (for example the energy law for collisionless ions or a mobility law in the collisional case), the spatial distribution of the field $\bar{E}(x)$, the potential $\bar{\Phi}(x)$ and the ion density $n_i(x)$ in the sheath can be explicitly found. Invoking the step model again finally yields the phase-resolved quantities $E(x, t)$ and $n_e(x, t)$ as well as the sheath voltage $V_{sh}(t)$.

However successful the step approximation is, it has a serious problem: it is realistic only in the range $x \ll s(t)$ where the electron density is small. For $x \gtrsim s(t)$ it becomes wrong: the true electric field does *not* vanish in this range, instead, it assumes the value of the ambipolar field $E = -\frac{T_e}{en_i}\frac{\partial n_i}{\partial x}$. Physically, this 'thermal' contribution is necessary to overcome the diffusion pressure $-\frac{\partial p_e}{\partial x}$ of the electrons in order to maintain quasi-neutrality $n_i \approx n_e$. (It would not be possible to employ Poisson's equation to calculate this field, as the charge density $\rho = e(n_i - n_e)$ is not exactly zero but only small compared with the values of en_i and en_e. An extended discussion of this point and the concept of quasi-neutrality in general can be found in the book by Chen [20]. There the simultaneous use of the assumptions $n_e = n_i$ and $\nabla \cdot \vec{E} \neq 0$ is referred to as the *plasma approximation*.)

Due to the failure of the step approximation for $x \gtrsim s$, the validity of all sheath models based on it is limited to the sheath *alone*: the transition to the bulk cannot be described. In fact, inconsistencies can only be prevented by introducing more or less artificial boundary conditions at the sheath edge s_{max}. The proper choice of these boundary conditions is anything but obvious, even in the stationary, near-collisionless case where everybody acknowledges the significance of the Bohm criterion [21]. A sometimes heated debate in the literature concerning the plasma sheath boundary bears witness to that [22–28].

This work aims to lay the ground for boundary sheath models which are more consistent. Its basis is a recent publication of this author, where the Boltzmann–Poisson equation was analysed using systematic two-scale analysis [29]. Identifying the 'fast' scale with the Debye length λ_D and the 'slow' scale with the sheath thickness $\bar{s}$, an approximate formal solution of the Boltzmann–Poisson equation was constructed which is asymptotically correct both in the depletion region and in the quasi-neutral zone. Starting from there, this paper will transform the unwieldy formal

solution of [29] into an algebraic form which can directly compete with the step model—while avoiding its pitfalls. Care is taken that the final formulae exhibit the same flexibility as the step model for the calculation of the phase averages, even when the modulation is not sinusoidal. (This situation applies not only for discharges which are excited by two or more power sources with different radio frequencies [30–34] but also for single frequency discharges where certain collective resonances can be excited by the nonlinearity of the sheath itself [7, 35–40].)

The rest of this work is organized as follows. In the next section, the model of a collisional, capacitive RF sheath introduced by Lieberman [2] will be revisited, and an exact numerical solution of it will be constructed as a reference. In section 3, this reference solution will be contrasted with the approximate solution that Lieberman himself gave using the step model. This concrete example will provide a good motivation for the subsequent more general investigations of section 4, where nothing more is assumed about the ion density than the scale relations $\lambda_D \frac{\partial n_i}{\partial x} \ll n_i$ and $\lambda_D^2 \frac{\partial^2 n_i}{\partial x^2} \ll n_i$. (These scale relations, together called the condition of *weak spatial variation*, are the local equivalent of the scale relation $\lambda_D \ll \bar{s}$.) Improved expressions for the instantaneous and phase-averaged field and electron density in such sheaths are derived which will be termed the *advanced algebraic approximation* (AAA). These expressions depend on the modulating RF current and the ion density distribution only in a purely algebraic way, and can easily be employed in further analytical work. Returning to the collisional sheath, section 5 will construct, as an a example, a sheath model based on the AAA and compare it with both the reference solution and with Lieberman's model. Section 6 ends the paper with a discussion.

2. The collisional capacitive sheath and its exact solution

In his publication of 1989, Lieberman considered the case of a capacitively driven RF sheath in the collisional limit [1]. In this regime—which applies when the gas pressure is higher than approximately 5 Pa—the ion mean free path λ_i is much smaller than the sheath width and ion inertia effects may be neglected. The ions are then drift-dominated, i.e. their velocity v_i is a function $v_i = \mu_i \bar{E}$ of the local phase-averaged electric field $\bar{E}$. This quantity is related to the instantaneous field $E(x,t)$ via ($T_{RF} = 2\pi/\omega_{RF}$):

$$\bar{E}(x) = \frac{1}{T_{RF}} \int_0^{T_{RF}} E(x,t)\,\mathrm{d}t. \tag{1}$$

Under the assumption of a constant mean free path λ_i, the mobility μ_i itself scales inversely with the speed. Together with an equation that describes the conservation of the ion flux Ψ_i (where ionization is neglected and the sign reflects that the x-axis points form the electrode at $x = 0$ into the bulk at $x \to \infty$), the collisional sheath model states that

$$n_i v_i = -\Psi_i, \tag{2}$$

$$v_i = \frac{2e\lambda_i}{|v_i| m_i \pi} \bar{E}. \tag{3}$$

The electrons, in contrast, follow the electrical field instantaneously. It can thus be assumed that they are in Boltzmann equilibrium, i.e. that their diffusion pressure $p_e = n_e T_e$ balances the electric force $-e n_e E$. For a constant electron temperature,

$$T_e \frac{\partial n_e}{\partial x} = -e n_e E. \tag{4}$$

The instantaneous electrical field is related to the charge density via Poisson's equation,

$$\epsilon_0 \frac{\partial E}{\partial x} = e(n_i - n_e). \tag{5}$$

The RF modulation is introduced by setting the total sheath current (a spatial constant) equal to a periodic function $j_{RF}(t)$. It is assumed that $j_{RF}(t)$ is harmonic with amplitude J_{RF} and frequency ω_{RF}, and that a possible dc contribution $\bar{j}$ vanishes. (The latter assumption is realistic for sheaths in front of insulators or capacitively blocked electrodes; the minus sign is merely convenient.)

$$\epsilon_0 \frac{\partial E}{\partial t} + j_e - e\Psi_i = j_{tot}(t) = -J_{RF} \sin(\omega_{RF} t). \tag{6}$$

The phase average of the electron current $j_e(t)$ is equal to the current $e\Psi_i$ of the ions. Assuming that electrons which reach the electrode are absorbed, the Hertz–Langmuir formula applies which equates the absorbed flux to the product of the local density times and the thermal speed times a numerical factor of order unity [22]:

$$\Psi_i = \frac{1}{T_{RF}} \int_0^{T_{RF}} \frac{1}{e} j_e \Big|_0 \,\mathrm{d}t = \sqrt{\frac{T_e}{2\pi m_e}} \frac{1}{T_{RF}} \int_0^{T_{RF}} n_e \,\mathrm{d}t \Big|_0. \tag{7}$$

Sheath-like solutions of the model equations are sought which exhibit electron depletion at finite x but become quasi-neutral for $x \to \infty$ with vanishing electrical field:

$$\lim_{x\to\infty} n_e - n_i = 0, \tag{8}$$

$$\lim_{x\to\infty} E = 0. \tag{9}$$

Under these conditions, the instantaneous sheath charge (more exactly, surface charge density per unit charge), typically a positive quantity, can be introduced:

$$Q(t) = \int_0^\infty n_i - n_e \,\mathrm{d}x. \tag{10}$$

For later comparison with the step models, it is useful to express the sheath charge also in terms of the equivalent electron edge $s(t)$, implicitly defined via

$$Q(t) = \int_0^{s(t)} n_i(x)\,\mathrm{d}x. \tag{11}$$

Integrating Poisson's equation from 0 to ∞ shows that Q is up to a factor $-e/\epsilon_0$ identical to the field at the electrode (which is therefore typically negative):

$$Q(t) = -\frac{\epsilon_0}{e} E\big|_0. \tag{12}$$

The charge is governed by the balance equation which is derived by evaluating the total current at $x = 0$ and $x \to \infty$:

$$\frac{\mathrm{d}Q}{\mathrm{d}t} = \frac{1}{e}\Big[e\Psi_\mathrm{i} - j_\mathrm{e}\Big]_0^\infty = \frac{J_\mathrm{RF}}{e}\sin(\omega_\mathrm{RF}t) - \Psi + \frac{1}{e}j_\mathrm{e}\Big|_0. \quad (13)$$

The quantity $j_\mathrm{e}|_0 - e\Psi_\mathrm{i}$ is average-free and typically much smaller than the RF current. It is therefore possible to neglect its contribution in the charge balance equation, which is then simplified to a purely harmonic form

$$\frac{\mathrm{d}Q}{\mathrm{d}t} = n_\mathrm{i}(s)\frac{\mathrm{d}s}{\mathrm{d}t} = \frac{J_\mathrm{RF}}{e}\sin(\omega_\mathrm{RF}t). \quad (14)$$

To write the equations in a non-dimensional form, certain parameter combinations are introduced, termed the reference density $\hat{n}$, the reference ion speed $\hat{v}$, the Debye length $\hat{\lambda}_\mathrm{D}$ and the ion drift time unit τ. In the following overview, the reference quantities are evaluated for the example given in [1], a 47 mTorr argon discharge with $\omega_\mathrm{RF} = 2\pi \times 13.56\,\mathrm{MHz}$, $e\Psi_\mathrm{i} = 0.5\,\mathrm{mA\,cm^{-2}}$, $J_\mathrm{RF} = 10.8\,\mathrm{mA\,cm^{-2}}$, $\lambda_\mathrm{i} = 0.07\,\mathrm{cm}$ and $T_\mathrm{e} = 3\,\mathrm{eV}$:

$$\hat{n} = \left(\frac{m_\mathrm{i}^2\pi^2\epsilon_0\Psi_\mathrm{i}^4}{4e^2T_\mathrm{e}\lambda^2}\right)^{1/5} \equiv 6.9\times10^9\,\mathrm{cm^{-3}}, \quad (15)$$

$$\hat{v} = \frac{\Psi_\mathrm{i}}{\hat{n}} = \left(\frac{4e^2T_\mathrm{e}\lambda^2\Psi_\mathrm{i}}{m_\mathrm{i}^2\pi^2\epsilon_0}\right)^{1/5} \equiv 4600\,\mathrm{m\,s^{-1}} \quad (16)$$

$$\hat{\lambda}_\mathrm{D} = \sqrt{\frac{\epsilon_0T_\mathrm{e}}{e^2\hat{n}}} = \left(\frac{2T_\mathrm{e}^3\epsilon_0^2\lambda}{e^4m_\mathrm{i}\pi\Psi_\mathrm{i}^2}\right)^{1/5} \equiv 1.6\times10^{-2}\,\mathrm{cm}, \quad (17)$$

$$\tau = \frac{\hat{\lambda}_\mathrm{D}}{\hat{v}} = \left(\frac{\pi m_\mathrm{i}T_\mathrm{e}^2\epsilon_0^3}{2e^6\lambda_\mathrm{i}\Psi_\mathrm{i}^3}\right)^{1/5} \equiv 3.4\times10^{-8}\,\mathrm{s}. \quad (18)$$

Furthermore, two dimensionless parameters are formed, called the electron loss ratio μ and the dimensionless RF current J:

$$\mu = \frac{\hat{v}}{\sqrt{T_\mathrm{e}/(2\pi m_\mathrm{e})}} \equiv 0.016, \quad (19)$$

$$J = \frac{J_\mathrm{RF}}{(e\hat{n}\hat{\lambda}_\mathrm{D}\omega_\mathrm{RF})} \equiv 7.4. \quad (20)$$

The normalization of the dynamical quantities is carried out by $x \to \hat{\lambda}_\mathrm{D}x$, $t \to t/\omega_\mathrm{RF}$, $n_\mathrm{i} \to \hat{n}\,n_\mathrm{i}$, $n_\mathrm{e} \to \hat{n}\,n_\mathrm{e}$, $v_\mathrm{i} \to \hat{v}v_\mathrm{i}$, $E \to (T_\mathrm{e}/e\hat{\lambda}_\mathrm{D})E$ and $Q \to \hat{\lambda}_\mathrm{D}\hat{n}Q$. (Here and in what follows, the dimensional and non-dimensional use of the symbols is distinguished by the context.) From the dimensionless system of equations, the ion density n_i and the velocity v_i can be eliminated in terms of the phase-averaged electrical field:

$$v_\mathrm{i} = -\frac{1}{n_\mathrm{i}} \equiv -\sqrt{-\bar{E}}, \quad (21)$$

$$n_\mathrm{i} = \frac{1}{\sqrt{-\bar{E}}}. \quad (22)$$

To express the electron density n_e and the field E, it is advantageous to introduce an electrical potential via $\Phi = \ln(n_\mathrm{e})$ and write

$$n_\mathrm{e} = \exp(\Phi), \quad (23)$$

$$E = -\frac{\partial\Phi}{\partial x}. \quad (24)$$

The dimensionless field model is then a nonlinear differential equation for Φ:

$$-\frac{\partial^2\Phi}{\partial x^2} = \frac{1}{\sqrt{-\bar{E}}} - \exp(\Phi), \quad (25)$$

subject to the boundary conditions

$$\frac{\partial\Phi}{\partial x}\Big|_0 = Q(t), \quad (26)$$

$$\lim_{x\to\infty}\exp(\Phi) - \frac{1}{\sqrt{-\bar{E}}} = 0. \quad (27)$$

The sheath charge is determined from its balance equation, together with the condition that the dc current vanishes:

$$\frac{\mathrm{d}Q}{\mathrm{d}t} = n_\mathrm{i}(s)\frac{\mathrm{d}s}{\mathrm{d}t} = J\sin(t)\Big|_0, \quad (28)$$

$$\frac{1}{2\pi}\int_0^{2\pi}\exp(\Phi)\,\mathrm{d}t\Big|_0 = \mu. \quad (29)$$

Finally, the phase-averaged field is related to the instantaneous potential by

$$\bar{E} = -\frac{1}{2\pi}\int_0^{2\pi}\frac{\partial\Phi}{\partial x}\,\mathrm{d}t. \quad (30)$$

It is advantageous to first construct a solution for the case without modulation ($J = 0$). The stationary collision-dominated sheath is described by an ordinary differential equation and its boundary conditions

$$\frac{\partial^2\Phi}{\partial x^2} = \frac{1}{\sqrt{\frac{\partial\Phi}{\partial x}}} - \exp(\Phi), \quad (31)$$

$$\lim_{x\to\infty}\exp(\Phi) - \frac{1}{\sqrt{\frac{\partial\Phi}{\partial x}}} = 0, \quad (32)$$

$$\exp(\Phi)\Big|_0 = \mu. \quad (33)$$

For large x, the solutions of the differential equation (31) under the condition (32) can be asymptotically expanded, up to an arbitrary translation $x \to x - c$:

$$\Phi \sim \frac{1}{2}\log\left(2x + \frac{2}{3}\sqrt{2}x^{-3/2} - \frac{83}{48}x^{-4} + \frac{20525}{1872\sqrt{2}}x^{-13/2} + \cdots\right). \quad (34)$$

An evolution at sufficiently large x provides a start for a numerical integration downwards. Condition (33) then determines $c = 3.108$. The particles densities and fields are displayed in figures 2 and 3, together with the asymptotics (dotted).

In the general case $J \neq 0$, the model amounts to a nonlinear integro-differential equation for a space and time dependent function $\Phi(x, t)$. A relaxation scheme was

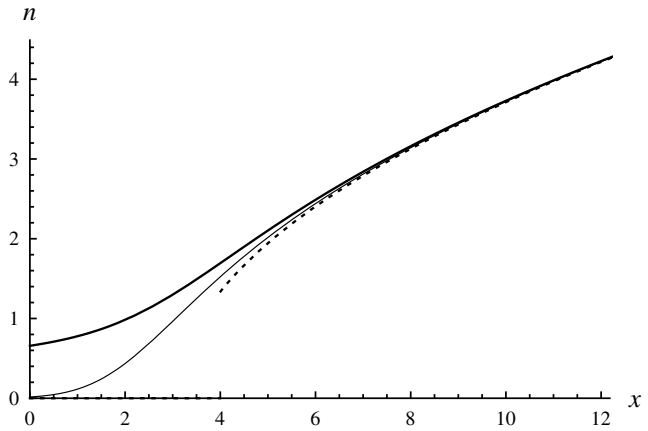

Figure 2. The ion density $n_i(x)$ (solid, thick) and the electron density $n_e(x)$ (solid, thin) of the stationary collision-dominated boundary sheath. The thick dotted line represents the leading term of the asymptotic expansion for large x.

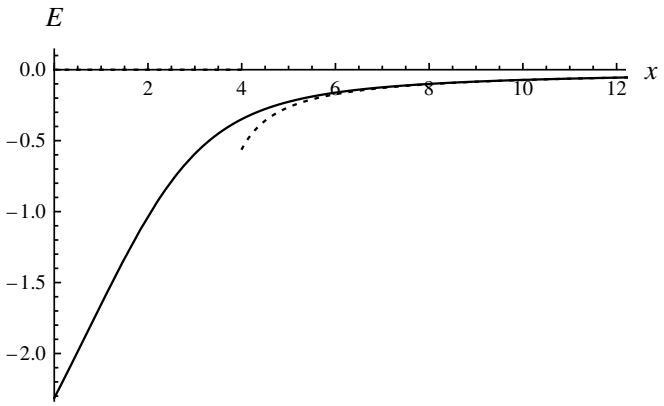

Figure 3. The electrical field $E(x)$ (solid) of the stationary collision-dominated boundary sheath. The thick dotted line represents the leading term of the asymptotic expansion for large x.

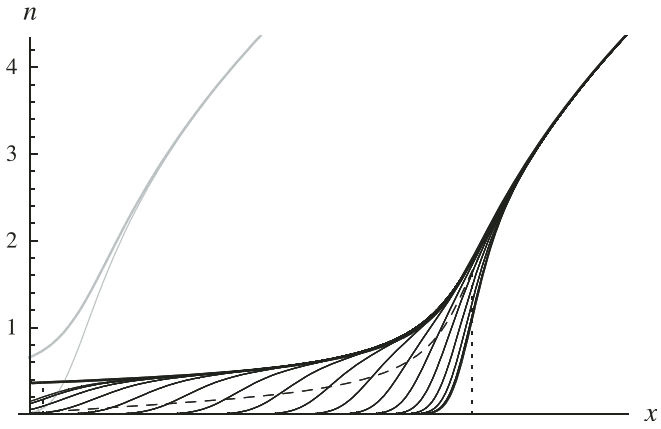

Figure 4. Particle densities of the RF driven collisional sheath at a modulation value of $J = 7.42$. Shown are the ion density $n_i(x)$ (thick) and the instantaneous electron densities $n_e(x, t)$ (thin) at various phases t between 0 and 2π. The average electron density $\bar{n}_e(x)$ is dashed. Also shown are the minimal and maximal values s_{min} and s_{max} of the equivalent electron edge. The light grey curves are the electron and ion densities of the unmodulated sheath.

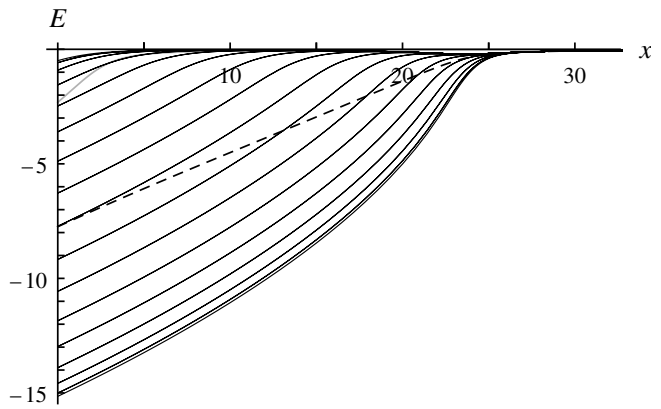

Figure 5. Field distribution of the RF driven collisional sheath at a modulation value of $J = 7.4$. Shown is the field strength $E(x, t)$ (solid) at various phases t between 0 and 2π, together with its phase average $\bar{E}(x)$ (dashed). The light grey curve gives the field of the unmodulated sheath.

employed to search for 2π-periodic solutions. Again, it turned out advantageous to first construct a solution without regard to the current condition and then perform a suitable translation $x \to x - c$. A finite interval $[x_{min}, x_{max}]$ was chosen so that x_{min} was well below the sheath minimum and x_{max} well above the maximum. The choices $x_{min} = -25$ and $x_{max} = 25$ proved appropriate. At x_{max}, quasi-neutrality (27) was imposed, at x_{min}, instead of (26), the modified condition $\frac{\partial \Phi}{\partial x}\big|_{x_{min}} = \bar{Q} - J\cos(t)$, where $\bar{Q}$ was an arbitrary (but suitably chosen) positive number. The interval was discretized into 250 cells of size $\Delta x = 0.2$; also the RF cycle $[0, 2\pi]$ was split into 64 intervals with $\Delta t = \pi/32$. Equations (25) and (30) were discretized using a finite difference scheme, with the endpoints $t = 0$ and $t = 2\pi$ identified. The discrete equations were then solved by a Newton relaxation scheme. Finally, the translation parameter c was determined to fulfil the phase-averaged current condition (29). Note that this guarantees the time-resolved current balance (28) as well, possibly except for a short time span during the 'sheath collapse' when the electron charge between x_{min} and 0 is not equal to zero. This deviation, however, can safely be neglected; similar errors were made in the derivation of (28) itself and in the definition of the equivalent electron step $s(t)$.

The relaxation scheme was run for current amplitudes increasing from $J = 0$ to $J = 10$. For $J = 0$, the dc model provided a start solution; for $J > 0$, the solution of the preceding run was employed. The results are shown for Lieberman's example $J = 7.4 \equiv 10.8\,\mathrm{mA\,cm^{-2}}$. Displayed are, in figure 4, the ion density $n_i(x)$ and the phase-averaged electron density $\bar{n}_e(x)$ together with the instantaneous electron density $n_e(x, t)$ for selected phases in steps of $2\pi/32$. Also indicated are the minimum s_{min} and the maximum s_{max} of the equivalent electron edge. Figure 5 shows the corresponding instantaneous and phase-averaged electrical fields.

The solutions exhibit sheath behaviour with electron depletion at the electrode and asymptotic quasi-neutrality for $x \to \infty$, where $n_i \sim \sqrt{2(x - c)}$ and $E \sim -1/(2(x - c))$. The size of the depletion region is phase-dependent. It nearly (but not exactly) vanishes at the 'sheath collapse' $t = 0$ and becomes maximal a half period later. The phase-averaged

electron density $\bar{n}_e$ grows slowly from near zero at the electrode to the value of n_i for $x \to \infty$. For any given t, however, the transition from electron depletion to quasi-neutrality takes place within a few λ_D around $s(t)$. The relative abruptness of this 'electron edge' in comparison with the total sheath width is, of course, the motivation for the step model.

3. The collisional sheath under the step approximation

Requiring the numerical treatment of a nonlinear integro-differential equation in x and t, the exact treatment of the collisional sheath was computationally costly. In his original work, Lieberman avoided that problem by invoking Godyak's step model approximation [1, 3]. This approach will now be recapitulated, using a slightly different path and the dimensionless notation of the last section. The step model approximates the fast but smooth transition from electron depletion to quasi-neutrality by a literal step at the electron edge $s(t)$,

$$n_e(x,t) = \begin{cases} 0 & x < s(t), \\ n_i(x) & x > s(t). \end{cases} \tag{35}$$

The location of the electron edge is related to the sheath charge by

$$Q(t) = \int_0^{s(t)} n_i(x)\,\mathrm{d}x, \tag{36}$$

its motion is described by the equation

$$\frac{\mathrm{d}Q}{\mathrm{d}t} = e n_i(s(t))\frac{\mathrm{d}s}{\mathrm{d}t} = J\sin(t). \tag{37}$$

In the step model, the Hertz–Langmuir formula is not applicable, the position of the electrode is instead identified with the minimum value of the sheath position,

$$s_{\min} = s(0) = 0. \tag{38}$$

This allows to integrate the sheath charge balance to

$$Q(t) = \int_0^{s(t)} n_i\,\mathrm{d}x = J - J\cos(t). \tag{39}$$

Inserting the step model into Poisson's equation, the field and the potential in the sheath can be calculated by integration, with the latter being measured relative to the bulk:

$$E(x,t) = \begin{cases} -\displaystyle\int_x^{s(t)} n_i(x')\,\mathrm{d}x' & x < s(t), \\ 0 & x > s(t), \end{cases} \tag{40}$$

$$\Phi(x,t) = \begin{cases} \displaystyle\int_x^{s(t)} (x-x')n_i(x')\,\mathrm{d}x' & x < s(t), \\ 0 & x > s(t). \end{cases} \tag{41}$$

The model is completed by expressing the ion density in terms of the average field:

$$n_i(x) = \frac{1}{\sqrt{-\bar{E}(x)}}. \tag{42}$$

Rearranging Lieberman's arguments slightly, it is noted that the electrical field and the sheath charge are both linear functions of the sheath density integral. This suggests to define a new spatial coordinate, termed the charge coordinate q, via

$$q(x) = \int_0^x n_i(x')\,\mathrm{d}x', \tag{43}$$

in terms of which the electrical field can expressed as

$$E(q,t) = \begin{cases} q - J + J\cos(t) & q < J - J\cos(t), \\ 0 & q > J - J\cos(t). \end{cases} \tag{44}$$

For coordinate values between 0 and $2J$, the phase average of the field is

$$\bar{E}(q) = \frac{1}{\pi}\left(\sqrt{(2J-q)\,q} - (q-J)\arccos\left(\frac{q}{J}-1\right)\right). \tag{45}$$

The ion density is consequently

$$n_i(q) = \frac{\sqrt{\pi}}{\sqrt{\sqrt{(2J-q)\,q} - (q-J)\arccos\,(q/J-1)}}. \tag{46}$$

The instantaneous electron density is

$$n_e(q,t) = \begin{cases} 0 & \\ \quad q < J - J\cos(t) & \\ \dfrac{\sqrt{\pi}}{\sqrt{\sqrt{(2J-q)\,q} - (q-J)\arccos\,(q/J-1)}} & \\ \quad q > J - J\cos(t) & \end{cases} \tag{47}$$

the corresponding phase average reads, for coordinate values between 0 and $2J$ as

$$\bar{n}_e(q) = \frac{\sqrt{\pi}\,(1 - \arccos(q/J-1)/\pi))}{\sqrt{\sqrt{(2J-q)\,q} - (q-J)\arccos\,(q/J-1)}}. \tag{48}$$

The step model thus allows to express the phase-averaged field $\bar{E}$, the ion density n_i and the phase-averaged electron density $\bar{n}_e$ as algebraic functions of the charge coordinate q. The phase-resolved values of the field E and the electron density n_e depend additionally on the phase t or, equivalently, on the instantaneous sheath charge $Q(t) = J(1+\cos(t))$. All expressions are local in q, i.e. they do not require the calculation of an integral or the solution of a differential equation. To recover from q the original spatial coordinate x, however, an integral must be computed:

$$\begin{aligned} x(q) &= \int_0^q \frac{1}{n_i(q')}\,\mathrm{d}q' \\ &= \frac{1}{\sqrt{\pi}}\int_0^{q/J} \sqrt{\sqrt{(2-\eta)\eta} - (\eta-1)\arccos(\eta-1)}\,\mathrm{d}\eta\, J^{3/2}. \end{aligned} \tag{49}$$

Figures 6 and 7 display the solutions of Lieberman's collisional sheath model for an RF modulation current of $J = 7.4$. The curves are thus directly comparable to their counterparts of the exact reference solution (which are shown as grey curves in the background). Qualitatively and quantitatively, the results are similar. The models agree on the thickness of the sheath, on the magnitude of the densities and the field and on the spatial distribution of those quantities.

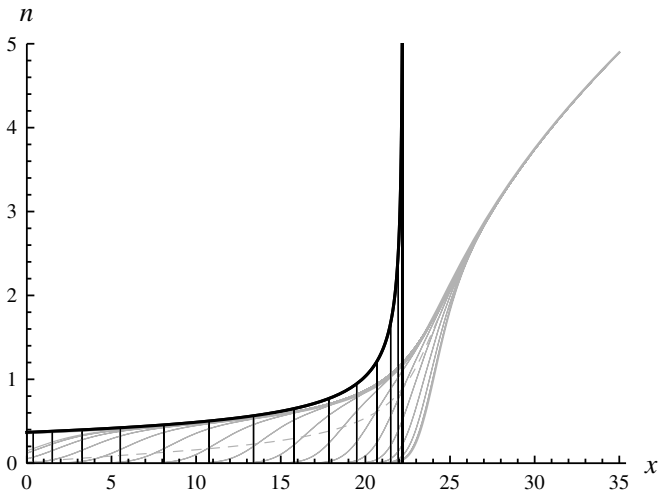

Figure 6. Densities of the collisional capacitive sheath under the step approximation for $J = 7.4$. The thick solid line denotes the ion density $n_i(x)$, the thin solid lines are the step-like electron densities $n_e(x, t)$ for different phases t. The dashed line denotes the average electron density $\bar{n}_e(x)$. The grey lines in the background show, for comparison, the corresponding densities $n_i(x)$, $n_e(x, t)$ and $\bar{n}_e(x)$ of the exact numerical solution.

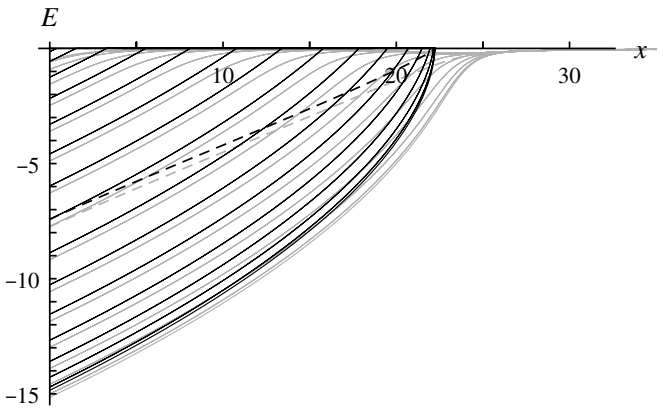

Figure 7. Electric field of the collisional capacitive sheath under the step approximation for $J = 7.4$. Shown is the field strength $E(x, t)$ (solid) at various phases t between 0 and 2π, together with its phase average $\bar{E}(x)$ (dashed). For comparison, the grey curves in the background show the corresponding fields $E(x, t)$ and $\bar{E}(x)$ of the exact numerical solution.

There are, however, also pronounced differences, all of which relate to the fact that the step model neglects thermal effects. Note that by itself the adoption of the step model seems uncritical. At any moment t the transition from electron depletion to quasi-neutrality is much steeper than the gradient of the ion density. To represent that transition by a step $s(t)$ located at the position of the equivalent electron edge (11) is quite reasonable. In a way, the deviations are due to indirect effects.

The first indirect effect concerns the location of the electrode. In the reference solution, the electrode position $x_E = 0$ is defined as the point where the current condition (29) holds. Owing to the smallness of the electron loss parameter μ, the electrode position is in general left of the minimum of the effective electron edge $s(t)$ (in the example, $x_E = 0$, $s_{min} = 0.71$). The step model, however, identifies the electrode position with that minimum, $x_E = s_{min} = 0$. This is the main cause of the deviation in the depletion region. A spatial translation of the Lieberman solution by $\Delta x = 0.71$ would lead to a much better agreement, but, of course, that parameter can only be determined in hindsight.

The second indirect effect appears at the sheath edge. The reference solution merges smoothly into the quasi-neutral solution where $n_e = n_i = \sqrt{2(x - c}$ and $E = -1/(2(x - c))$, of course driven by the ambipolar field. The step model, on the other hand, does not include the ambipolar field and instead gives $E \to 0$ for $x \to s_{max}$. Lieberman's sheath model is therefore terminated at s_{max} by a divergence in the densities. This implies not only that it cannot be self-consistently matched to a bulk model. It also has the effect that the sheath becomes nearly 10% thinner—compare the value $s_{max} = 22.2$ of the Lieberman model with the corresponding value $s_{max} = 24.1$ of the reference solution.

4. The advanced algebraic approximation

The step model has the advantage of leading to an algebraic representation of the phase-resolved and phase-averaged values of the electrical field $E(q)$ and the electron density $n_e(q)$. However, it covers only the depletion zone and fails in the quasi-neutral zone. Reference [29] studied the situation in detail. An improved approximation was derived which is similar to that of the step model, in the sense that it assumes the existence of a suitable (positive and non-decreasing) ion density $n_i(x)$ and constructs an approximate sheath-like solution of the Boltzmann–Poisson equation

$$-\frac{\partial^2 \Phi}{\partial^2 x} = n_i(x) - \exp(\Phi). \tag{50}$$

In contrast to the step model, the improved representation uses no ad hoc assumptions but is based on a systematic asymptotic expansion in the regime of weak spatial variation, $\lambda_D \frac{\partial n_i}{\partial x} \ll n_i$ and $\lambda_D^2 \frac{\partial^2 n_i}{\partial x^2} \ll n_i$, where λ_D is the normalized electron Debye length $\lambda_D = 1/\sqrt{n_i}$. (In other words, it is based on a two-scale analysis where the 'fast' scale is the Debye length and the 'slow' scale is the sheath width.) The approximation reads (with $d_1 \approx 0.388$) as

$$\Phi(x, s) = \begin{cases} \displaystyle\int_x^s (x - x') n_i(x')\, \mathrm{d}x' + \ln(n_i(s)) & x < s \\ \displaystyle -1 + d_1 \frac{\lambda_D(s)}{n_i(s)} \frac{\partial n_i}{\partial s} & \\ \ln(n_i(x)) & x > s \end{cases} \tag{51}$$

$$+\Delta\Psi_0\left(\frac{x - s}{\lambda_D(s)}\right) + \frac{\lambda_D(s)}{n_i(s)} \frac{\partial n_i}{\partial s} \Delta\Psi_1\left(\frac{x - s}{\lambda_D(s)}\right),$$

while the corresponding field is

$$E(x, s) = \begin{cases} \displaystyle -\int_x^s n_i(x')\, \mathrm{d}x & x < s \\ \displaystyle -\frac{1}{n_i} \frac{\partial n_i}{\partial x} & x > s \end{cases}$$

$$-\frac{1}{\lambda_D(s)} \Delta\Psi_0'\left(\frac{x - s}{\lambda_D(s)}\right) - \frac{1}{n_i(s)} \frac{\partial n_i}{\partial s} \Delta\Psi_1'\left(\frac{x - s}{\lambda_D(s)}\right). \tag{52}$$

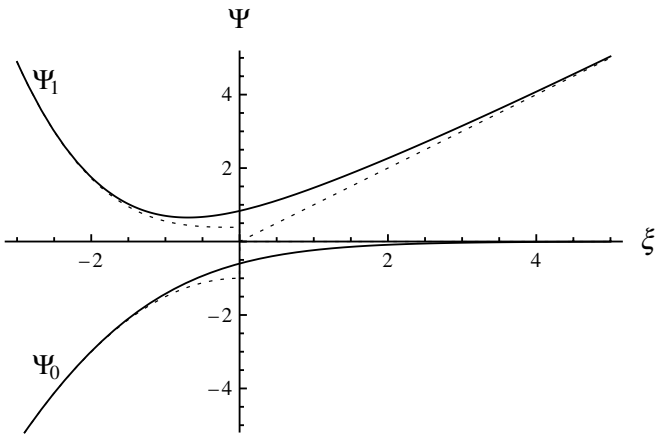

Figure 8. The characteristic sheath functions $\Psi_0(\xi)$ and $\Psi_1(\xi)$ in dependence on their argument ξ. The dotted curves are the asymptotics of polynomial form for $\xi \ll 0$ and $\xi \gg 0$, respectively.

The parameter s denotes the location of the 'equivalent electron edge' and is defined so that the field behaves for negative x asymptotically like the step model for the same s:

$$\lim_{x\to-\infty} E(x,s) + \int_x^s n_\mathrm{i}(x')\,\mathrm{d}x = 0. \tag{53}$$

The symbol $\lambda_\mathrm{D}(s)$ denotes the normalized Debye length evaluated at s:

$$\lambda_\mathrm{D}(s) = \frac{1}{\sqrt{n_\mathrm{i}(s)}}. \tag{54}$$

The characteristic functions Ψ_0 and Ψ_1 are shown in figure 8. They are the unique solutions of the following differential equations and asymptotic boundary conditions, where $d_0 = -1$ and $d_1 \approx 0.388$ are nonlinear eigenvalues which ensure the prescribed polynomial behaviour for large values of $|\xi|$:

$$-\frac{\partial^2\Psi_0}{\partial\xi^2} + e^{\Psi_0} = 1, \quad \Psi_0 \to \begin{cases} d_0 - \dfrac{1}{2}\xi^2 & \xi \ll 0, \\ 0 & \xi \gg 0, \end{cases} \tag{55}$$

$$-\frac{\partial^2\Psi_1}{\partial\xi^2} + e^{\Psi_0}\Psi_1 = \xi, \quad \Psi_1 \to \begin{cases} d_1 - \dfrac{1}{6}\xi^3 & \xi \ll 0, \\ \xi & \xi \gg 0. \end{cases} \tag{56}$$

The functions $\Delta\Psi_0$ and $\Delta\Psi_1$ used in the representation of the potential are defined from the Ψ_0 and Ψ_1 by subtracting the respective polynomial asymptotics for $\xi < 0$ and $\xi > 0$. By construction, they vanish quickly for large values of $|\xi|$. The functions $\Delta\Psi_0'$ and $\Delta\Psi_1'$ are the piecewise derivatives of $\Delta\Psi_0$ and $\Delta\Psi_1$, with the discontinuities at $\xi = 0$ not considered. They also vanish for large values of $|\xi|$.

The improved field representation has several advantages. It is asymptotically correct both in the depletion zone (for $x \ll s - \lambda_\mathrm{D}(s)$) and in the quasi-neutral zone (for $x \gg s + \lambda_\mathrm{D}(s)$). It also describes the transition quite faithfully: the expression is continuous and correct up to linear order in the small parameter $\frac{\lambda_\mathrm{D}}{n_\mathrm{i}}\frac{\partial n_\mathrm{i}}{\partial x}$, all errors contain either the square of that parameter or the quadratically small factor $\frac{\lambda_\mathrm{D}^2}{n_\mathrm{i}}\frac{\partial^2 n_\mathrm{i}}{\partial x^2}$. In [29], a numerical study was performed for a realistic model density. The outcome showed that the maximal deviation of the improved field representation from the exact solution of the Boltzmann–Poisson equation is in the percentage range.

In the form given above, the field representation is not yet suitable for practical work: the field at a point x does not only depend on the value of x itself but also on the position of the sheath edge s and on the yet unknown ion density $n_\mathrm{i}(x)$ in the interval in between. This, however, is exactly the same problem that the step model field had, and it is suggestive to try the same remedy: a transformation of the field representation from the spatial parameters x and s to the charge coordinates q and Q. As it will turn out, this approach indeed solves the problem, but only for the electrical field E, not for the electrical potential Φ. For that reason, the discussion will now be restricted to the field, the situation for the potential will be discussed later—i.e. it will be explained why the approach fails.

It will prove advantageous to define the charge coordinates q and Q in a slightly more general way as above, by replacing 0 by a (initially unspecified) reference point $\bar{s}$:

$$q = \int_{\bar{s}}^{x} n_\mathrm{i}(x)\,\mathrm{d}x, \tag{57}$$

$$Q = \int_{\bar{s}}^{s} n_\mathrm{i}(x)\,\mathrm{d}x \equiv q(s). \tag{58}$$

Both the depletion field and the ambipolar field can be transformed without any problems. For the transition terms it suffices to invoke an approximation: the $\Delta\Psi'(\xi)$ vanish quickly for large $|\xi|$, so that all functions of $s = s(Q)$ may be represented by a Taylor expansion around the point $Q = q$ (of an order consistent with that of the field representation itself). For the argument ξ itself, the following relation holds where the quadratic term in the expansion is not neglected but vanishes exactly:

$$\xi = \frac{x-s}{\lambda_\mathrm{D}(s)} = \frac{q-Q}{\sqrt{n_\mathrm{i}}} + O\left((Q-q)^3\right). \tag{59}$$

The Taylor expansions of the pre-factors read as

$$\frac{1}{\lambda_\mathrm{D}(s)} = \sqrt{n_\mathrm{i}} - \frac{1}{2}\frac{1}{\sqrt{n_\mathrm{i}}}\frac{\partial n_\mathrm{i}}{\partial q}(q-Q) + O\left((Q-q)^2\right), \tag{60}$$

$$\frac{1}{n_\mathrm{i}(s)}\frac{\partial n_\mathrm{i}}{\partial s} = \frac{\partial n_\mathrm{i}}{\partial q} + O\left(Q-q\right). \tag{61}$$

Collecting the results, the approximate expression of the field is

$$\begin{aligned} E(q,Q) = {} & \begin{cases} q-Q & q < Q \\ -\dfrac{\partial n_\mathrm{i}}{\partial q} & q > Q \end{cases} \\ & - \left(\sqrt{n_\mathrm{i}} - \frac{q-Q}{2\sqrt{n_\mathrm{i}}}\frac{\partial n_\mathrm{i}}{\partial q}\right)\Delta\Psi_0'\left(\frac{q-Q}{\sqrt{n_\mathrm{i}}}\right) \\ & - \frac{\partial n_\mathrm{i}}{\partial q}\Delta\Psi_1'\left(\frac{q-Q}{\sqrt{n_\mathrm{i}}}\right). \end{aligned} \tag{62}$$

A closer examination shows that the explicit case distinction in (62) and those embodied in the definition of the $\Delta\Psi'$ cancel; the cases $q < Q$ and $q > Q$ lead to the same expressions. It is

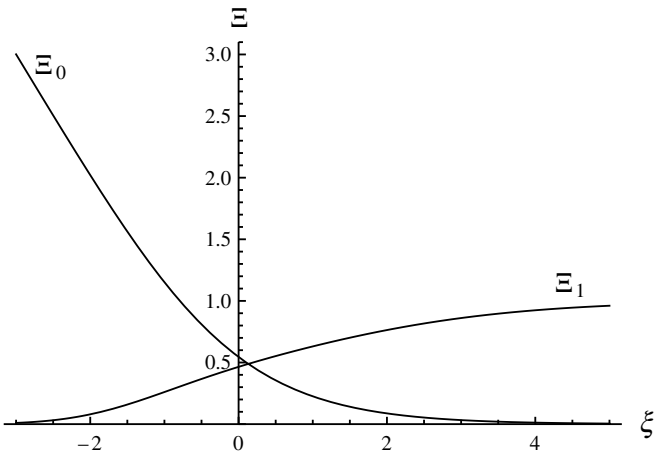

Figure 9. The sheath functions $\Xi_0(\xi)$ and $\Xi_1(\xi)$ in dependence on the argument ξ.

advantageous to define two new characteristic functions $\Xi_0(\xi)$ and $\Xi_1(\xi)$, see figure 9:

$$\Xi_0(\xi) = \Psi_0'(\xi), \tag{63}$$

$$\Xi_1(\xi) = \Psi_1'(\xi) - \frac{\xi}{2}\Psi_0'(\xi). \tag{64}$$

In terms of these functions, the phase-resolved electrical field E can be expressed as an algebraic function of its arguments q, n_i, $n_\mathrm{i}' \equiv \frac{\partial n_\mathrm{i}}{\partial q}$, and Q:

$$E\left(q, n_\mathrm{i}, n_\mathrm{i}', Q\right) = -\Xi_0\left(\frac{q-Q}{\sqrt{n_\mathrm{i}}}\right)\sqrt{n_\mathrm{i}} - \Xi_1\left(\frac{q-Q}{\sqrt{n_\mathrm{i}}}\right)\frac{\partial n_\mathrm{i}}{\partial q}. \tag{65}$$

This expression has a number of interesting features. It is *local*, i.e. the field at the point q depends only on the ion density and its derivative at that point; the sheath charge state Q appears as a parameter. It is *quasi-linear*, i.e. the dependence on the derivative is linear, with a pre-factor that is a function of the density. The explicit dependence on the charge coordinate q and the sheath charge Q appears as the difference $q - Q$; this ensures *translation invariance* with respect to the reference point $\bar{s}$. (In other words, it is possible to specify the origin of the q-coordinates at discretion; this degree of freedom will be advantageous later.) The representation is *analytical*, all derivatives with respect to q exist (provided, of course, that the ion density n_i is a smooth function of q).

It is suggestive to think of Ξ_0 and Ξ_1 as 'switch functions' which control the physical character of the field: for $q - Q \ll -\sqrt{n_\mathrm{i}}$, in the unipolar zone, $\Xi_0(\xi) \to -\xi$ and $\Xi_1(\xi) \to 0$, this recovers the depletion field. For $q - Q \gg \sqrt{n_\mathrm{i}}$, in the ambipolar zone, $\Xi_0(\xi) \to 0$ and $\Xi_1(\xi) \to 1$ yield the ambipolar field. The transition takes place in the zone $|q - Q| \lesssim \sqrt{n_\mathrm{i}}$, here the field is reasonable but not exact. The model error, the absolute deviation between the approximate and the exact field, scales with $n_\mathrm{i}'^2/\sqrt{n_\mathrm{i}}$ and $\sqrt{n_\mathrm{i}}n_\mathrm{i}''$. (In the depletion zone, the model error vanishes exponentially, in the quasi-neutral zone it behaves like $n_\mathrm{i}n_\mathrm{i}'''$ which is the error of the ambipolar field expression itself.)

It is, unfortunately, not possible to construct an algebraic representation with similar properties for the electrical potential. The problem stems from the depletion region $x \ll s$, where the potential behaves like $\int_s^x (x' - x)n_\mathrm{i}(x')\,\mathrm{d}x'$. Transformed in the charge coordinates, this term would read as $\int_Q^q \int_q^{q'} \frac{1}{n_\mathrm{i}(q'')}\,\mathrm{d}q''\,\mathrm{d}q'$ which is not local but depends explicitly on the ion density between q and Q. (In other words the 'mathematical trick' of transforming the explicit dependence on $n_\mathrm{i}(x)$ away only works once. It was employed for $\int n_\mathrm{i}(x')\,\mathrm{d}x'$ and cannot be used again for $\int (x - x')n_\mathrm{i}(x')\,\mathrm{d}x'$.) Luckily, it will turn out later that the discussed situation poses no real difficulties; the potential needs to be calculated only after the ion density n_i(q) is *explicitly* available. In that situation, one may use the integral

$$\Phi(q) = \ln\left(n_\mathrm{i}(q)\right) + \int_\infty^q \sqrt{n_\mathrm{i}(q')}\,\Xi_0\left(\frac{q'-Q}{\sqrt{n_\mathrm{i}(q')}}\right) + \frac{\partial n_\mathrm{i}}{\partial q'}\left(\Xi_1\left(\frac{q'-Q}{\sqrt{n_\mathrm{i}(q')}}\right) - 1\right)\frac{1}{n_\mathrm{i}(q')}\,\mathrm{d}q'.$$

This formula can be verified by checking that it (i) is asymptotically correct in the ambipolar limit $q \to \infty$ and (ii) obeys the differential equation

$$E(q, Q) = -n_\mathrm{i}(q)\frac{\partial}{\partial q}\Phi(q, Q). \tag{66}$$

For the electron density, the situation is more advantageous: in spite of the fact that this quantity depends directly on the potential, one can construct a local algebraic representation. Consider the function $\hat{\Phi}(x, s)$ which is simply the potential expression $\Phi(x, s)$ valid for $x > s$ extended to the whole domain,

$$\hat{\Phi}(x, s) = \ln(n_\mathrm{i}(x)) + \Psi_0\left(\frac{x-s}{\lambda_\mathrm{D}(s)}\right) + \frac{\lambda_\mathrm{D}(s)}{n_\mathrm{i}(s)}\frac{\partial n_\mathrm{i}}{\partial s}\left(\Psi_1\left(\frac{x-s}{\lambda_\mathrm{D}(s)}\right) - \frac{x-s}{\lambda_\mathrm{D}(s)}\right). \tag{67}$$

By construction, $\hat{\Phi}$ is identical to Φ for $x > s$. For x which are smaller but still close to s, the difference can be expressed as a Taylor series around s that starts with a quadratic term. This results, of course, from the construction of the potential approximation (51):

$$\hat{\Phi}(x, s) - \Phi(x, s) \approx \frac{n_\mathrm{i}'(s)^2 - n_\mathrm{i}(s)n_\mathrm{i}''(s)}{2n_\mathrm{i}(s)^2}(x - s)^2. \tag{68}$$

Under the assumption of weak spatial variation of the ion density, the potential difference is thus negligible as long as $x \gtrsim s - \lambda_\mathrm{D}$. For $x < s - \lambda_\mathrm{D}$, the potential difference becomes larger, both expressions diverge to minus infinity on different paths. The exponential applied to $\hat{\Phi}$ is thus identical to the electron density for $x > s$, differs only slightly for $s - \lambda_\mathrm{D} \leqslant x < s$ and converges again to it, i.e. to zero, for $x \lesssim s - \lambda_\mathrm{D}$. In other words, $\exp(\hat{\Phi})$ is a good representation of n_e for all values of x. Transformed into the charge coordinates q and Q, approximated for weak spatial variation and expressed in terms

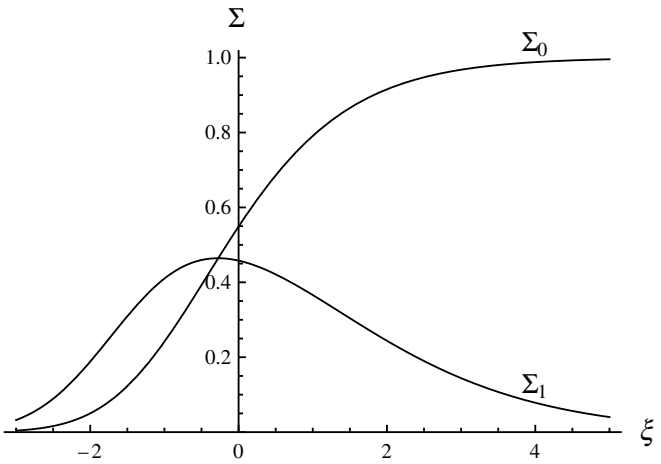

Figure 10. The sheath functions $\Sigma_0(\xi)$ and $\Sigma_1(\xi)$ in dependence on the argument ξ.

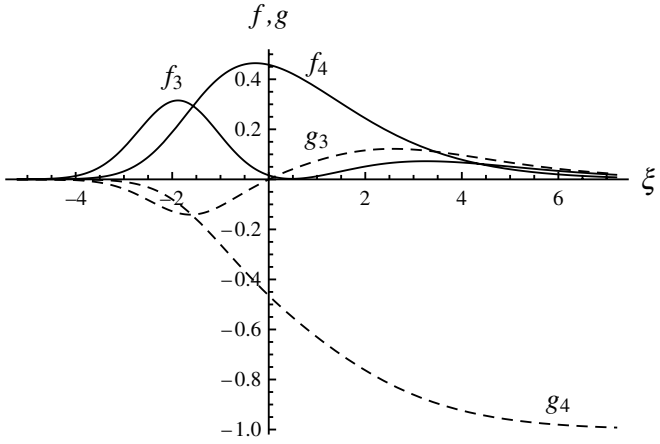

Figure 11. The error coefficients $f_3(\xi)$, $f_4(\xi)$ of the Boltzmann equilibrium (solid) and $g_3(\xi)$, $g_4(\xi)$ of the Poisson equation (dashed) as functions of their argument ξ.

of two new analytical functions $\Sigma_0(\xi)$ and $\Sigma_1(\xi)$ defined as (see figure 10)

$$\Sigma_0(\xi) = \exp\left(\Psi_0(\xi)\right), \tag{69}$$

$$\Sigma_1(\xi) = \exp\left(\Psi_0(\xi)\right)\left(\Psi_1(\xi) - \xi\right), \tag{70}$$

the approximate expression of the electron density n_e reads as

$$n_e(q, n_i, n_i', Q) = \Sigma_0\left(\frac{q-Q}{\sqrt{n_i}}\right) n_i + \Sigma_1\left(\frac{q-Q}{\sqrt{n_i}}\right)\sqrt{n_i}\,\frac{\partial n_i}{\partial q}. \tag{71}$$

Verification shows that this expression is indeed asymptotically correct. For $q - Q \ll -\sqrt{n_i}$, $\Sigma_0(\xi) \to 0$ and $\Sigma_1(\xi) \to 0$; this lets n_e vanish. For $q - Q \gg \sqrt{n_i}$, $\Sigma_0(\xi) \to 1$ and $\Sigma_1(\xi) \to 0$, and quasi-neutrality follows. (Note, however, that the stated asymptotic correctness refers only to the absolute deviation of the model (71) from the exact solution. The relative error of the two quantities behaves differently: it vanishes for $q - Q \gg \sqrt{n_i}$ but not for $q - Q \ll -\sqrt{n_i}$. In the unipolar zone, both the true electron density and the algebraic model (71) vanish exponentially but their ratio does not tend to unity.)

The following analysis is meant to give some background on the mathematical foundation of the representation. Consider the task of representing the electrical field E and the electron density n_e by expressions that are local in q and n_i, depend explicitly on the sheath charge Q and are consistent with the assumption of weak spatial variation. Clearly, these expressions may be general functions of $q - Q$ and $n_i(q)$, must be linear in n_i' and cannot depend on higher derivatives of n_i. Without loss of generality, they may hence be written as (65) and (71), with the ansatz functions Ξ_0, Ξ_1, Σ_0 and Σ_1 depending on $(q - Q)/\sqrt{n_i(q)}$ and additionally, for the moment, on $n_i(q)$ as a second argument. Inserting the expressions into Poisson's equation and the Boltzmann equilibrium and sorting terms yields the following, where the functions f_k and g_k, $k = 1 \ldots 4$, are certain combinations of the ansatz functions and their derivatives that depend on $\xi = (q - Q)/\sqrt{n_i}$ and $n_i(q)$:

$$n_i\frac{\partial n_e}{\partial q} + E n_e = f_1 n_i^{3/2} + f_2 n_i\frac{\partial n_i}{\partial q} + f_3\, n_i^{1/2}\left(\frac{\partial n_i}{\partial q}\right)^2 + f_4\, n_i^{3/2}\frac{\partial^2 n_i}{\partial q^2}, \tag{72}$$

$$n_i\frac{\partial E}{\partial q} - n_i + n_e = g_1\, n_i + g_2\, n_i^{1/2}\frac{\partial n_i}{\partial q} + g_3\left(\frac{\partial n_i}{\partial q}\right)^2 + g_4\, n_i\frac{\partial^2 n_i}{\partial q^2}. \tag{73}$$

In the regime of small spatial variation, the last two terms of the equations are neglected. Poisson's equation and Boltzmann equilibrium are thus approximately valid if (and only if) the coefficients f_1, f_2, g_1 and g_2 are identically zero. A closer investigation reveals that this is only possible when the ansatz functions follow the definitions (63), (64), (69) and (70) together with the differential equations (55) and (56). In particular, the ansatz functions must be independent of $n_i(q)$; i.e. the original representations (65) and (71) were general enough. The remaining functions f_3, f_4, g_3 and g_4 are then determined; see figure 11:

$$f_3(\xi) = \tfrac{1}{2}\exp\big(\Psi_0(\xi)\big)\big(-2\Psi_1(\xi)\Psi_1'(\xi) + \xi\,\Psi_1'(\xi) + \Psi_1(\xi)\big), \tag{74}$$

$$f_4(\xi) = \exp\big(\Psi_0(\xi)\big)\big(\Psi_1(\xi) - \xi\big), \tag{75}$$

$$g_3(\xi) = -\tfrac{1}{4}\xi\big(\Psi_0'(\xi) - 2\exp\big(\Psi_0(\xi)\big)\Psi_1(\xi) + \xi\exp\big(\Psi_0(\xi)\big) + \xi\big), \tag{76}$$

$$g_4(\xi) = \tfrac{1}{2}\xi\Psi_0'(\xi) - \Psi_1'(\xi). \tag{77}$$

These residual functions are bounded for all ξ and one concludes that Poisson's equation and Boltzmann's equilibrium are indeed valid for weak spatial variation of the ion density. (Note, however, that $f_3(\xi)$ and $f_4(\xi)$ are not bounded for $\xi \to \infty$ when divided by $\exp(\Psi_0(\xi))$; this is another indication that the relative error of the electron density in the depletion region, i.e. the ratio of the model density to the true density, may be possibly large.)

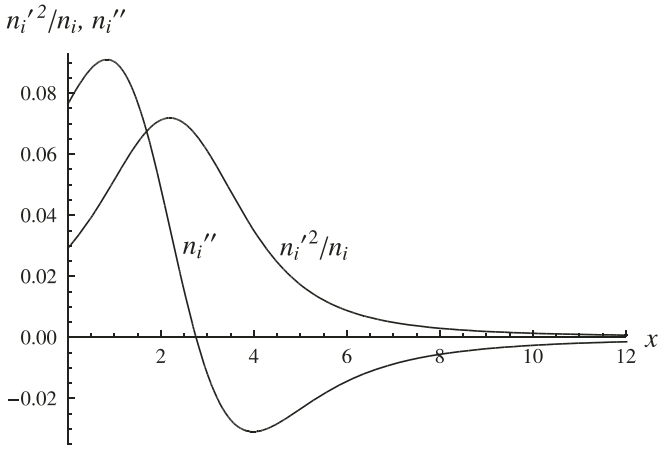

Figure 12. The measures $n_i'(q)^2/n_i(q)$ and $n_i''(q)$ of the spatial variation of the ion density $n_i(q)$ of the stationary sheath, displayed over the coordinate x. The variation is largest in the transition zone and smaller in the depletion and quasi-neutral regions. The upper bound of about 10% for the two measures demonstrates that the ion density distribution of the stationary collisional sheath has indeed a weak spatial variation. This holds for boundary sheaths in general.

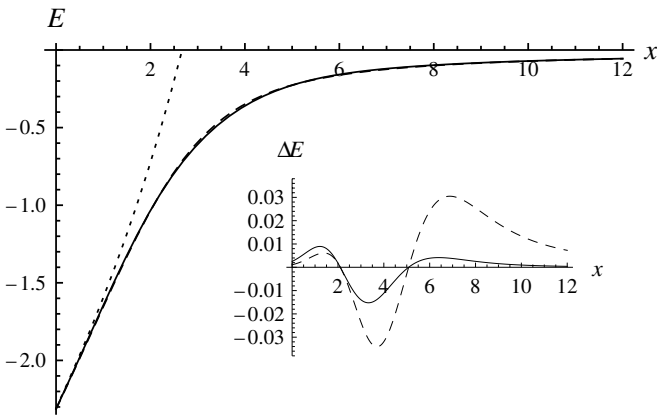

Figure 13. Approximate representation (65) of the electrical field $E(x)$, evaluated with the ion density of the stationary collisional sheath (solid), compared with the exact field of that model (dashed). Also shown is the field predicted by the step model (dotted). The inset shows the absolute (solid) and the relative error (dashed) which are in the percentage range.

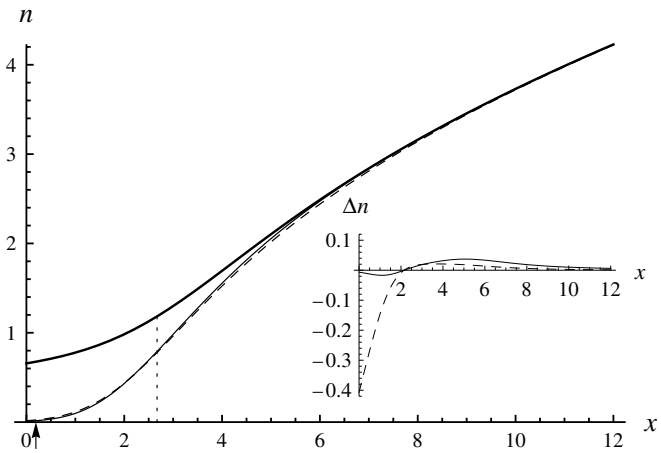

Figure 14. Approximate representation (71) of the electron density $n_e(x)$, evaluated with the ion density $n_i(x)$ of the stationary collisional sheath model (thick), compared with the exact electron density $n_e(x)$ of that model (dashed). Also shown is the electron density of the step model (dotted). The inset shows the absolute error which is in the percentage range, and the relative error which becomes large in the depletion region $x \ll s$. The arrow indicates the location of the electrode when calculated with the approximate instead of the exact electron density.

As a test, the improved algebraic approximation will now be evaluated numerically for the example of the stationary collisional sheath—equations (31)–(33), displayed in figures 2 and 3. The ion density $n_i(x)$ of that model is employed as a given function of weak spatial variation. Figure 12 displays the absolute variation measures $n_i'^2/n_i$ and n_i'' and demonstrates that they are indeed small compared with unity, namely below 10%. (Note that the variation measures are functions of q and that the prime denotes a derivative with respect to that variable. To facilitate comparison, however, the quantities are plotted over the true spatial coordinate. Of course, there is an explicit relation to the variation measures directly expressed in x, namely $n_i'^2/n_i = (\frac{\lambda_D}{n_i}\frac{\partial n_i}{\partial x})^2$ and $n_i'' = \frac{\lambda_D^2}{n_i}\frac{\partial^2 n_i}{\partial x^2} - (\frac{\lambda_D}{n_i}\frac{\partial n_i}{\partial x})^2$, with $\lambda_D = 1/\sqrt{n_i}$.)

Figure 13 shows the electrical field calculated by the algebraic model, in comparison with the reference field and also the field of the step approximation. It can be seen that the deviation of the algebraic representation from the reference field is absolutely and relatively very small. The absolute error of the field is less than 0.01 in dimensionless units; the relative error is never larger than 3%. Also the absolute error in the electron density is small, see figure 14. (However, as expected, the relative error increases for $x \to 0$. To illustrate the consequences, the arrow shows where the current condition $\bar{n}_e = \mu$ is met for the algebraic electron density. The deviation from the exact position $x_E = 0$ gives rise to a sheath thickness error of 7%.) Finally, figure 15 shows the relative residuals of Poisson's equation and Boltzmann's relation. The first residual is always smaller than 0.02, it quickly vanishes outside the transition region. The second residual reaches values up to 0.1. This is another indication that the relative error of the electron density is not necessarily small.

Finally, it will now be shown that it is possible to derive algebraic representations also for the time-averaged field and electron density. The construction is based on the fact that the algebraic representation is local and that it depends on the RF modulation only via $Q(t)$. In the following, the expressions before the equivalent sign assume an arbitrary 2π-periodicity (often more realistic [7, 30–40]), the expressions after it hold for sinusoidal RF:

$$\frac{\mathrm{d}Q}{\mathrm{d}t} = J(t) \equiv J\sin(t). \tag{78}$$

To render the solution of this equation unique, the integration constant is chosen so that the sheath charge $Q(t)$ has a vanishing phase average; this is always achievable by re-defining the origin $\bar{x}$ of the sheath coordinates:

$$Q(t) = \int_0^t J(t')\,\mathrm{d}t' + \frac{1}{2\pi}\int_0^{2\pi} t' J(t')\,\mathrm{d}t' \equiv -Q\cos(t). \tag{79}$$

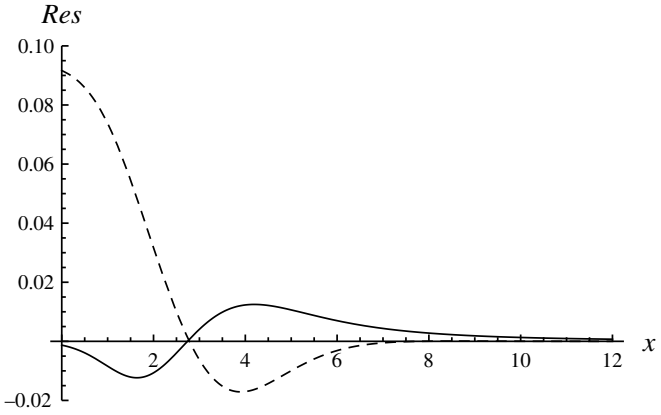

Figure 15. Relative residuum of Poisson's equation (solid) and the Boltzmann equilibrium (dashed) when evaluated with the approximate dc field strength and electron density, as a function of x. The residuum of Poisson's equation is always smaller than 0.02; the residuum of the Boltzmann relation assumes a value of nearly 0.1 at the electrode.

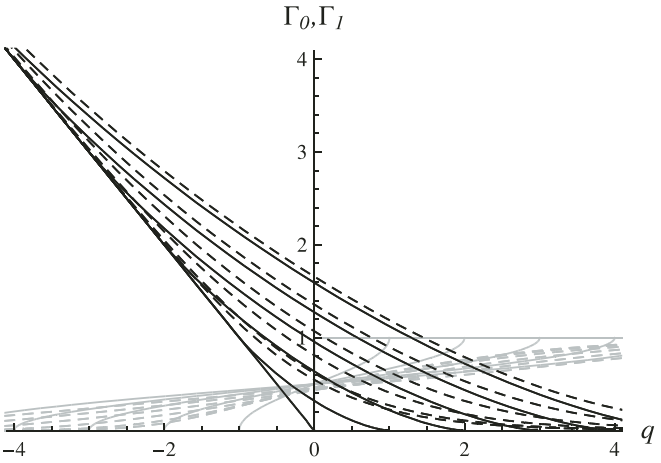

Figure 16. Characteristic functions Γ_0 (black) and Γ_1 (grey) for $n_\mathrm{i} = 0$ (solid) and $n_\mathrm{i} = 1$ (dashed). The RF modulation is sinusoidal, $J = J\cos(t)$, with amplitudes $J = 0\ldots5$. For $n_\mathrm{i} = 0$ and $J = 0$, $\Gamma_0 = -q\theta(-q)$ and $\Gamma_1 = \theta(q)$. For finite n_i and J, the functions are spread by the modulation ∼J and smoothed by thermal effects $\sim\sqrt{n_\mathrm{i}}$.

On the basis of the 'phase-resolved switch functions' Ξ_0 and Ξ_1, two 'phase-averaged switch functions' Γ_0 and Γ_1 are now defined which depend on q, the local ion density $n_\mathrm{i}(q)$ and on the function $Q(t)$ (or the amplitude J):

$$\Gamma_0\left(q, n_\mathrm{i}, \{Q\}\right) = \sqrt{n_\mathrm{i}}\frac{1}{2\pi}\int_0^{2\pi}\Xi_0\left(\frac{q-Q(t)}{\sqrt{n_\mathrm{i}}}\right)\mathrm{d}t \equiv \sqrt{n_\mathrm{i}}\frac{1}{2\pi}\int_0^{2\pi}\Xi_0\left(\frac{q+J\cos(t)}{\sqrt{n_\mathrm{i}}}\right)\mathrm{d}t, \tag{80}$$

$$\Gamma_1\left(q, n_\mathrm{i}, \{Q\}\right) = \frac{1}{2\pi}\int_0^{2\pi}\Xi_1\left(\frac{q-Q(t)}{\sqrt{n_\mathrm{i}}}\right)\mathrm{d}t \equiv \frac{1}{2\pi}\int_0^{2\pi}\Xi_1\left(\frac{q-J\cos(t)}{\sqrt{n_\mathrm{i}}}\right)\mathrm{d}t. \tag{81}$$

For the case of a sinusoidal modulation, examples of the functions are displayed in figure 16. They act indeed as switches, with the abruptness of the switching behaviour

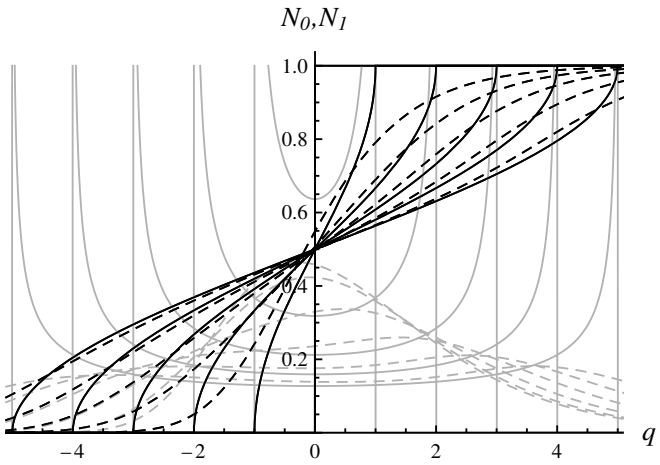

Figure 17. Characteristic functions N_0 (black) and N_1 (grey) for $n_\mathrm{i} = 0$ (solid) and $n_\mathrm{i} = 1$ (dashed). The RF modulation is sinusoidal, $J = J\cos(t)$, with amplitudes $J = 0\ldots5$.For $n_\mathrm{i} = 0$ and $J = 0$, $N_0 = \theta(q)$ and $\Gamma_1 = 2\delta(q)$. For finiten_i and J, the functions are spread by the modulation ∼J and smoothed by thermal effects $\sim\sqrt{n_\mathrm{i}}$.

controlled by the RF modulation and by thermal effects. In terms of these functions, the phase-averaged electrical field can be given as

$$\bar{E}(q, n_\mathrm{i}, n_\mathrm{i}', \{Q\}) = -\Gamma_0\left(q, n_\mathrm{i}, \{Q\}\right) - \frac{\partial n_\mathrm{i}}{\partial q}\,\Gamma_1\left(q, n_\mathrm{i}, \{Q\}\right). \tag{82}$$

By construction, the asymptotic behaviour of this expression recovers the depletion field for $q \ll Q_\mathrm{min} - \sqrt{n_\mathrm{i}}$ and the ambipolar field for $q \gg Q_\mathrm{max} + \sqrt{n_\mathrm{i}}$:

$$\bar{E}(q, n_\mathrm{i}, n_\mathrm{i}', \{Q\}) \to \begin{cases} q & q \ll Q_\mathrm{min} - \sqrt{n_\mathrm{i}}, \\ -\dfrac{\partial n_\mathrm{i}}{\partial q} & q \gg Q_\mathrm{max} + \sqrt{n_\mathrm{i}}. \end{cases} \tag{83}$$

Similar functions of q, n_i and functionals of $Q(t)$, termed N_0 and N_1, are defined on the basis of Σ_0 and Σ_1, they are displayed in figure 17:

$$N_0\left(q, n_\mathrm{i}, \{Q\}\right) = \frac{1}{2\pi}\int_0^{2\pi}\Sigma_0\left(\frac{q-Q(t)}{\sqrt{n_\mathrm{i}}}\right)\mathrm{d}t \equiv \frac{1}{2\pi}\int_0^{2\pi}\Sigma_0\left(\frac{q+J\cos(t)}{\sqrt{n_\mathrm{i}}}\right)\mathrm{d}t, \tag{84}$$

$$N_1\left(q, n_\mathrm{i}, \{Q\}\right) = \frac{1}{\sqrt{n_\mathrm{i}}}\frac{1}{2\pi}\int_0^{2\pi}\Sigma_1\left(\frac{q-Q(t)}{\sqrt{n_\mathrm{i}}}\right)\mathrm{d}t \equiv \frac{1}{\sqrt{n_\mathrm{i}}}\frac{1}{2\pi}\int_0^{2\pi}\Sigma_1\left(\frac{q+J\cos(t)}{\sqrt{n_\mathrm{i}}}\right)\mathrm{d}t. \tag{85}$$

These functions allow to express the phase-averaged electron density

$$\bar{n}_e(q) = n_\mathrm{i}\,\Sigma_0\left(q, n_\mathrm{i}, \{Q\}\right) - n_\mathrm{i}\frac{\partial n_\mathrm{i}}{\partial q}\,\Sigma_1\left(q, n_\mathrm{i}, \{Q\}\right). \tag{86}$$

Again, the asymptotic behaviour of this expression is consistent with the expectations:

$$\bar{n}_\mathrm{e}(q, n_\mathrm{i}, n_\mathrm{i}', \{Q\}) \to \begin{cases} 0 & q \ll Q_\mathrm{min} - \sqrt{n_\mathrm{i}}, \\ n_\mathrm{i} & q \gg Q_\mathrm{max} + \sqrt{n_\mathrm{i}}. \end{cases} \tag{87}$$

Together, formulae, (65, (71), (82) and (86), together with the definitions they depend on, will be referred to as the *advanced algebraic representation* (AAA) of the time-resolved and the time-averaged electrical field and electron density in an RF modulated sheath.

5. The collisional capacitive RF sheath under the AAA

The collisional, capacitive RF sheath will now be analysed again, this time under the AAA. The modulation is again sinusoidal, $Q = -J\cos(t)$. Inserting the expression for the average field into the ion equation of motion leads to

$$\frac{\partial n_\mathrm{i}}{\partial q}\,\Gamma_1\,(q, n_\mathrm{i}, J) = \frac{1}{n_\mathrm{i}^2} - \Gamma_0\,(q, n_\mathrm{i}, J)\,. \tag{88}$$

This equation can easily be solved, using the following procedure: for sufficiently negative q, the function Γ_1 vanishes and $\Gamma_0 \approx -q$. The equation then becomes algebraic and, in fact, identical to the so-called collisional Child–Langmuir model with field-dependent mobility. A suitably chosen point on this solution may be taken as a start for an integration of (88) into the positive q direction. Combining both solutions gives the ion density $n_\mathrm{i}(q)$ for all q. The average electrical field can then be recovered as

$$\bar{E}(q) = -\frac{1}{n_\mathrm{i}(q)^2}. \tag{89}$$

The average electron density is given as

$$\bar{n}_\mathrm{e}(q) = N_0\,(q, n_\mathrm{i}(q), J)\;n_\mathrm{i}(q) + N_1\,(q, n_\mathrm{i}(q), J)\,n_\mathrm{i}(q)\frac{\partial n_\mathrm{i}}{\partial q}. \tag{90}$$

The phase-resolved electrical field is

$$E(q,t) = -\Xi_0\left(\frac{q + J\cos(t)}{\sqrt{n_\mathrm{i}(q)}}\right)\sqrt{n_\mathrm{i}(q)} - \Xi_1\left(\frac{q + J\cos(t)}{\sqrt{n_\mathrm{i}(q)}}\right)\frac{\partial n_\mathrm{i}}{\partial q}, \tag{91}$$

the corresponding electron density reads as

$$n_\mathrm{e}(q,t) = \Sigma_0\left(\frac{q + J\cos(t)}{\sqrt{n_\mathrm{i}(q)}}\right)n_\mathrm{i}(q) + \Sigma_1\left(\frac{q + J\cos(t)}{\sqrt{n_\mathrm{i}(q)}}\right)\sqrt{n_\mathrm{i}(q)}\,\frac{\partial n_\mathrm{i}}{\partial q}. \tag{92}$$

The electrode is located at the position q_E where the current condition is met, $\bar{n}_\mathrm{e}(q_\mathrm{E}) = \mu$. The original spatial coordinate can then be recovered via the integral representation

$$x(q) = \int_{q_\mathrm{E}}^{q}\frac{1}{n_\mathrm{i}(q')}\,\mathrm{d}q'. \tag{93}$$

The sheath voltage, measured from q_E to a point q_B well in the quasi-neutral zone, is

$$V_\mathrm{sh}(t) = \int_{q_\mathrm{E}}^{q_\mathrm{B}}\left(\Xi_0\left(\frac{q' + J\cos(t)}{\sqrt{n_\mathrm{i}(q')}}\right)\sqrt{n_\mathrm{i}(q')} + \Xi_1\left(\frac{q' + J\cos(t)}{\sqrt{n_\mathrm{i}(q')}}\right)\frac{\partial n_\mathrm{i}}{\partial q'}\right)\frac{1}{n_\mathrm{i}(q')}\,\mathrm{d}q'. \tag{94}$$

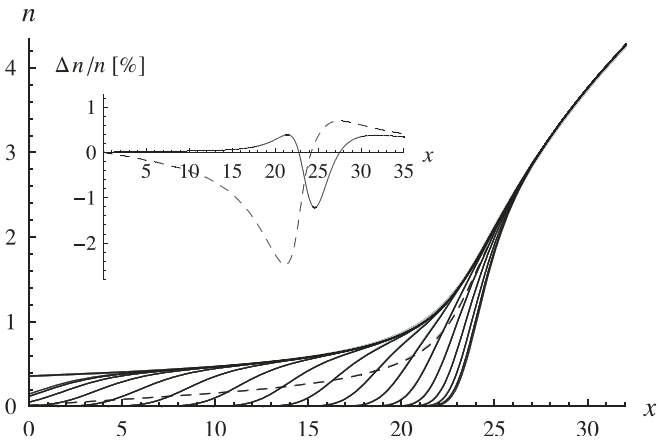

Figure 18. Particle densities of the collision-dominated sheath for an RF modulation of $J = 7.4$, calculated with the AAA. The thick solid line is the ion density $n_\mathrm{i}(x)$, the thin solid lines are the electron densities $n_\mathrm{e}(x, t)$ for different phases. The dashed line denotes the average electron density $\bar{n}_\mathrm{e}(x)$. The (for the most part occluded) grey lines show the corresponding densities of the exact numerical solution.

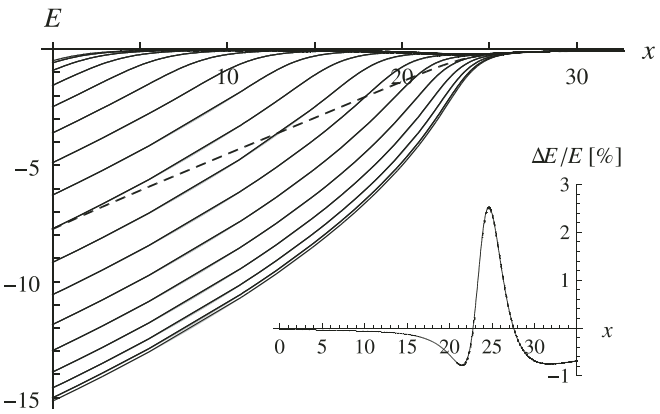

Figure 19. Electrical field E of the collision-dominated sheath for an RF modulation of $J = 7.4$, calculated with the AAA. Displayed is $E(x, t)$ for selected phases t, the dashed line denotes the phase average $\bar{E}(x)$. The (for the most part occluded) grey lines show the corresponding fields of the exact numerical solution. The inset displays the relative error of the approximation of the average field.

These equations were evaluated for the set of parameters used in sections 2 and 3. The result of the calculations is shown in figures 18 (particle densities) and 19 (electrical field). In both quantities, the agreement of the exact and the approximate solution is excellent. The absolute deviations are smaller than the thickness of the curves; the relative deviations (shown in the insets) are localized and never larger than a few per cent.

The AAA does not only capture the transition from electron depletion to quasi-neutrality in a realistic way but also cures the two 'indirect effects' which were mainly responsible for the shortcomings of the step model. Firstly, the position of the electrode is identified more accurately. (The large relative error of the electron density in the depletion region had no negative influence. For the discussed example, this is not surprising, the value $\bar{n}_\mathrm{e}|_{x_\mathrm{E}}$ is dominated by the contributions during the sheath collapse where $Q(t) \approx q_\mathrm{E}$. According to further numerical experiments, the error is larger for smaller

RF modulations but remains tolerable even for a dc sheath; see also figure 14.) Secondly, the divergence of the densities at the sheath edge $s_{\max}$ has disappeared, the model now merges smoothly into the ambipolar solution. This allows to consistently match the sheath model to a bulk model. Also, the thickness of the sheath is calculated much more realistically.

6. Summary and conclusion

Plasma boundary sheaths exhibit a gradual transition from electron depletion ($n_e \ll n_i$) to quasi-neutrality ($n_e \approx n_i$). In radio frequency plasmas, the transition is controlled both by the RF modulation and by thermal effects. Step models which neglect the latter are restricted to strongly modulated sheaths ($V_{RF} \gg T_e/e$) and fail when this condition is not met. This paper gave an improved analysis of the sheath–bulk transition which accounts for both influences simultaneously. The main results, which together are referred to as the advanced algebraic approximation (AAA), are now summarized in physical units.

It was assumed from the outset that the sheath dynamics can be described in a one-dimensional Cartesian geometry $x > 0$, with $x_E = 0$ denoting the position of the electrode. Sheath-like solutions were studied that are asymptotically quasi-neutral, $n_e \to n_i$ for $x \to \infty$. For mathematical reasons, it proved advantageous to employ also a second set of coordinates, termed the charge coordinates. In the definition of the spatial variable q, the parameter $\bar{s}$ denotes the average position of the effective electron edge $s(t)$:

$$q(x) = \int_{\bar{s}}^{x} n_i(x)\,\mathrm{d}x. \tag{95}$$

The instantaneous state of the sheath is given by the sheath charge $Q(t)$; it is defined by a relation which also implicitly defines the effective electron edge $s(t)$:

$$Q(t) = \int_{\bar{s}}^{\infty} n_i(x) - n_e(x)\,\mathrm{d}x = \int_{\bar{s}}^{s(t)} n_i\,\mathrm{d}x. \tag{96}$$

The sheath charge is modulated by the given RF current $J(t)$ which is assumed to be periodic but not necessarily sinusoidal:

$$\frac{\mathrm{d}Q}{\mathrm{d}t} = \frac{1}{e}J(t). \tag{97}$$

Because of the choice of the point $\bar{s}$, the sheath charge is phase-average free and reads as

$$Q(t) = \frac{1}{e}\left(\int_0^t J(t')\,\mathrm{d}t' + \frac{1}{T}\int_0^T t' J(t')\,\mathrm{d}t'\right). \tag{98}$$

The electrical field E and electron density n_e can be represented in a local algebraic form; Ξ_0, Ξ_1, Σ_0 and Σ_1 are analytical functions which act as 'switches':

$$E\left(q, n_i, n_i', Q\right) = -\Xi_0\left(\frac{e(q-Q)}{\sqrt{\epsilon_0 T_e n_i}}\right)\sqrt{\frac{T_e n_i}{\epsilon_0}} - \Xi_1\left(\frac{e(q-Q)}{\sqrt{\epsilon_0 T_e n_i}}\right)\frac{T_e}{e}\frac{\partial n_i}{\partial q}, \tag{99}$$

$$n_e\left(q, n_i, n_i', Q\right) = \Sigma_0\left(\frac{e(q-Q)}{\sqrt{\epsilon_0 T_e n_i}}\right) n_i + \Sigma_1\left(\frac{e(q-Q)}{\sqrt{\epsilon_0 T_e n_i}}\right)\frac{\sqrt{\epsilon_0 T_e n_i}}{e}\frac{\partial n_i}{\partial q}. \tag{100}$$

An algebraic expression for the phase-averaged field was constructed in terms of Γ_0 and Γ_1 which are functionals of $Q(t)$ but local functions of q and the ion density n_i:

$$\Gamma_0\left(q, n_i, \{Q\}\right) = \frac{1}{T}\int_0^T \Xi_0\left(\frac{e(q-Q(t))}{\sqrt{\epsilon_0 T_e n_i}}\right)\mathrm{d}t\,\frac{\sqrt{\epsilon_0 T_e n_i}}{e}, \tag{101}$$

$$\Gamma_1\left(q, n_i, \{Q\}\right) = \frac{1}{T}\int_0^T \Xi_1\left(\frac{e(q-Q(t))}{\sqrt{\epsilon_0 T_e n_i}}\right)\mathrm{d}t. \tag{102}$$

In terms of these functions, the phase-averaged electrical field is

$$\bar{E}(q, n_i, n_i', \{Q\}) = -\frac{e}{\epsilon_0}\Gamma_0\left(q, n_i, \{Q\}\right) - \frac{T_e}{e}\frac{\partial n_i}{\partial q}\,\Gamma_1\left(q, n_i, \{Q\}\right). \tag{103}$$

Similarly, two more sheath functions N_0 and N_1 were defined:

$$N_0\left(q, n_i, \{Q\}\right) = \frac{1}{T}\int_0^T \Sigma_0\left(\frac{e(q-Q(t))}{\sqrt{\epsilon_0 T_e n_i}}\right)\mathrm{d}t, \tag{104}$$

$$N_1\left(q, n_i, \{Q\}\right) = \frac{1}{T}\int_0^T \Sigma_1\left(\frac{e(q-Q(t))}{\sqrt{\epsilon_0 T_e n_i}}\right)\mathrm{d}t\,\frac{e}{\sqrt{\epsilon_0 T_e n_i}}, \tag{105}$$

in terms of which the phase-averaged electron density $\bar{n}_e$ reads as

$$\bar{n}_e(q, n_i, n_i', \{Q\}) = n_i N_0\left(q, n_i, \{Q\}\right) + \frac{\epsilon_0 T_e n_i(q)}{e^2}\frac{\partial n_i}{\partial q}\,N_1\left(q, n_i, \{Q\}\right). \tag{106}$$

These expressions are generalizations of the corresponding expressions of the step model. When thermal effects are neglected, i.e. in the limit $T_e \to 0$, the electrical field and the electron density assume the form of the step model:

$$E^{(\mathrm{step})}\left(q, Q\right) = \begin{cases} \dfrac{e(q-Q)}{\epsilon_0} & q < Q, \\ 0 & q > Q, \end{cases} \tag{107}$$

$$n_e^{(\mathrm{step})}\left(q, n_i, Q\right) = \begin{cases} 0 & q < Q, \\ n_i & q > Q. \end{cases} \tag{108}$$

Under the additional assumption of a harmonic modulation, $Q(t) = -(J/e\omega_{RF})\cos(\omega_{RF}t)$, and under the restriction on the range $|q| < J/\omega_{RF}$, the formulae of section 3 are recovered, except that the notation is now dimensional, and that Q is shifted by $J/e\omega_{RF}$:

$$\bar{E}^{(\mathrm{step})}\left(q, J\right) = \frac{1}{\pi}\frac{e}{\epsilon_0}\left(q\arccos\left(\frac{e\omega_{RF}q}{J}\right) - \sqrt{(J/e\omega_{RF})^2 - q^2}\right), \tag{109}$$

$$\bar{n}_e^{(\mathrm{step})}\left(q, n_i, J\right) = \left(1 - \frac{1}{\pi}\arccos\left(\frac{e\omega_{RF}q}{J}\right)\right) n_i. \tag{110}$$

The AAA allows to calculate the phase averages of the field and the electron density in an RF modulated sheath without more than local knowledge of the ion density and its derivative. When coupled to a similarly local model of the ion motion, an ordinary differential equation for the sheath results,

not a partial differential equation. This was demonstrated for the collisional sheath, where the ion model consists of the equation of continuity and the drift equation under the condition of a constant mean free path:

$$n_\mathrm{i} v_\mathrm{i} = -\Psi_\mathrm{i}, \tag{111}$$

$$v_\mathrm{i} = \frac{2e\lambda_\mathrm{i}}{|v_\mathrm{i}| m_\mathrm{i}\pi}\bar{E}. \tag{112}$$

The resulting differential equation is

$$\frac{T_\mathrm{e}}{e}\Gamma_1\left(q, n_\mathrm{i}, \{Q\}\right)\frac{\partial n_\mathrm{i}}{\partial q} = \frac{\pi m_\mathrm{i}\Psi_\mathrm{i}^2}{2e\lambda_\mathrm{i}}\frac{1}{n_\mathrm{i}^2} - \frac{e}{\epsilon_0}\Gamma_0\left(q, n_\mathrm{i}, \{Q\}\right). \tag{113}$$

When the sheath differential equation is solved, the charge coordinate position q_E of the electrode can be determined from the current balance

$$\sqrt{\frac{T_\mathrm{e}}{2\pi m_\mathrm{e}}}\left(N_0\left(q, n_\mathrm{i}(q), \{Q\}\right) n_\mathrm{i}(q) + N_1(q, n_\mathrm{i}(q), \{Q\})\frac{\epsilon_0 T_\mathrm{e} n_\mathrm{i}(q)}{e^2}\frac{\partial n_\mathrm{i}}{\partial q}\right)\Bigg|_{q=q_\mathrm{E}} = \Psi_\mathrm{i}. \tag{114}$$

The origin of the physical coordinates is located at the electrode, $x_\mathrm{E} = 0$. For other points, the spatial coordinate x is given by the formula

$$x(q) = \int_{q_\mathrm{E}}^{q}\frac{1}{n_\mathrm{i}(q')}\,\mathrm{d}q'. \tag{115}$$

For the electrical potential Φ, a local algebraic representation could not be constructed. Instead, its calculation requires the explicit knowledge of the ion density distribution $n_i(q)$ and can only be carried out after the sheath equation is solved:

$$\Phi(q,t) = \frac{T_\mathrm{e}}{e}\ln\left(\frac{n_\mathrm{i}(q)}{\hat{n}}\right) + \int_\infty^q\left(\sqrt{\frac{T_\mathrm{e} n_\mathrm{i}(q')}{\epsilon_0}}\,\Xi_0\left(\frac{e(q'-Q(t))}{\sqrt{\epsilon_0 T_\mathrm{e} n_\mathrm{i}(q')}}\right) + \frac{T_\mathrm{e}}{e}\frac{\partial n_\mathrm{i}}{\partial q'}\left(\Xi_1\left(\frac{e(q'-Q(t))}{\sqrt{\epsilon_0 T_\mathrm{e} n_\mathrm{i}(q')}}\right) - 1\right)\right)\frac{1}{n_\mathrm{i}(q')}\,\mathrm{d}q. \tag{116}$$

Correspondingly, also the sheath voltage can only be expressed in integral form:

$$V_\mathrm{sh}(t) = \int_{q_\mathrm{E}}^{q_\mathrm{B}}\left(\sqrt{\frac{T_\mathrm{e} n_\mathrm{i}(q')}{\epsilon_0}}\,\Xi_0\left(\frac{e(q'-Q(t))}{\sqrt{\epsilon_0 T_\mathrm{e} n_\mathrm{i}(q')}}\right) + \frac{T_\mathrm{e}}{e}\frac{\partial n_\mathrm{i}}{\partial q'}\,\Xi_1\left(\frac{e(q'-Q(t))}{\sqrt{\epsilon_0 T_\mathrm{e} n_\mathrm{i}(q')}}\right)\right)\frac{1}{n_\mathrm{i}(q')}\,\mathrm{d}q. \tag{117}$$

The AAA is based on the same idea as the step model. The central assumption is that of a weak spatial variation of the ion density or, equivalently, that of the relative abruptness of the transition from electron depletion to quasi-neutrality. The difference lies in the way that this assumption is utilized: the AAA avoids any ad hoc neglections and instead employs the systematic method of matched asymptotic expansions.

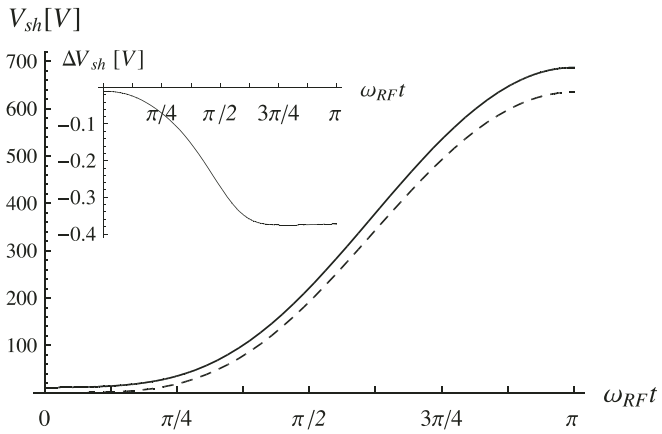

Figure 20. The voltage over the collisional sheath, calculated with the set of reference parameters. The dashed line corresponds to the step model solution of Lieberman, the solid black and grey lines—not distinguishable—are the exact solution and the solution under the advanced algebraic approximation. The inset shows the difference of the two.

The outcome is quite satisfactory: the AAA overcomes the problems of the step model, namely the miscalculation of the electrode position and the divergence at the sheath edge, and gives a more faithful representation of the sheath. At the same time, its final formulae are only slightly more complicated (admittedly, that does not hold for their derivation).

The main concern of this work was the mathematical consistency of the new formalism, not the achieved numerical accuracy. Nonetheless, the experiments conducted with the collisional capacitive sheath were quite convincing. Consider, as the last example, figure 20 which shows the overall sheath voltages V_sh in physical units. The step model (Lieberman's theory) differs considerably from the reference model, while the AAA exhibits an error of less than 0.4 V or 0.05%. Considering the level of accuracy which is usually obtainable in plasma physics, one may state that the AAA is essentially exact.

Finally, it remains to mention that the results presented in this paper have already found use in several applications. Kratzer *et al* have presented a hybrid model for the calculation of ion distribution functions behind a dc or RF driven plasma boundary sheath [41]. Sabisch *et al* have extended that model to calculate also the fluxes of energetic neutrals to exposed surfaces in the process of magnetically enhanced reactive ion etching (MERIE) [42]. Heil *et al* augmented the tool by a kinetic electron module and analysed the processes of Ohmic and stochastic heating in RF-CCPs [43, 44]. Schulze *et al* studied the phenomena experimentally and found good agreement between simulations and measurements [45, 46]. Recently, Heil *et al* studied the so-called electrical asymmetry effect with the same tool [47]. More work is currently under preparation.

Acknowledgments

The author gratefully acknowledges the support by the Deutsche Forschungsgemeinschaft via the Forschergruppe 1123 'Physics of Microplasmas' and valuable discussions

within the Graduiertenkolleg 1051 'Nonequilibrium phenomena in low-temperature plasmas'.

References

[1] Lieberman M A 1989 *IEEE Trans. Plasma Sci.* **17** 338
[2] Lieberman M A 1988 *IEEE Trans. Plasma Sci.* **16** 638
[3] Godyak V A and Ghanna Z K 1979 *Sov. J. Plasma Phys.* **6** 372
[4] Godyak A V and Sternberg N 1990 *Phys. Rev.* A **42** 2299
[5] Wild C and Koidl P 1991 *J. Appl. Phys.* **69** 2909
[6] Börnig K 1992 *Appl. Phys. Lett.* **60** 1553
[7] Klick M 1996 *J. Appl. Phys.* **79** 34445
[8] Kawamura E, Vahedi V, Lieberman M A and Birdsall C K 1999 *Plasma Sources Sci. Technol.* **8** R45
[9] Sobolewski M A 2000 *Phys. Rev.* E **62** 8540
[10] Qiu H T, Wang Y N and Ma T C 2001 *J. Appl. Phys.* **90** 5884
[11] Dewan M N A, McNally P J and Herbert P A F 2002 *J. Appl. Phys.* **91** 5604
[12] Robiche J, Boyle P C, Turner M M and Ellingboe A R 2003 *J. Phys. D: Appl. Phys.* **26** 1810
[13] Denpoh K, Wakayama G and Nanbu K 2004 *Japan. J. Appl. Phys.* **43** 5533
[14] Boyle P C, Robiche J and Turner M M 2004 *J. Phys. D: Appl. Phys.* **37** 1451—8
[15] Xiang N and Waelbroeck F L 2005 *J. Appl. Phys.* **95** 860
[16] Xiang N and Waelbroeck F L 2005 *J. Vac. Sci. Technol.* A **23** 23
[17] Jiang W, Mao M and Wang Y 2006 *Phys. Plasmas* **13** 113502
[18] Olevanov M, Proshina O, Rakhimova T and Voloshin D 2008 *Phys. Rev.* E **78** 026404
[19] Vallinga P M, Meijer P M, Deutsch H and de Hoog F J 1986 *Proc. 18th Int. Conf. on Phenomena in Ion Gases (Swansea, UK)* ed W T Williams (Bristol, UK: Hilger) p 814
[20] Chen F F 1984 *Introduction to Plasma Physics and Controlled Fusion* (New York: Plenum)
[21] Bohm D 1955 *The Characteristics of Electric Discharges in Magnetic Fields* ed A Guthrie and R Wakerling (New York: McGraw Hill)
[22] Riemann K-U 1989 *J. Appl. Phys.* **65** 999
[23] Godyak V A and Sternberg N 1990 *Phys. Rev.* A **42** 2299
[24] Riemann K-U 1991 *J. Phys. D: Appl. Phys.* **24** 493
[25] Godyak V A *et al* 1993 *IEEE Trans. Plasma Sci.* **21** 378
[26] Riemann K-U 2001 *J. Tech. Phys.* **41** 89
[27] Sternberg N and Godyak V 2003 *IEEE Trans. Plasma Sci.* **31** 665
[28] Riemann K-U *et al* 2005 *Plasma Phys. Control. Fusion* **47** 1949–70
[29] Brinkmann R P 2007 *J. Appl. Phys.* **102** 093303
[30] Goto H H, Löwe H D and Ohmi T 1992 *J. Vac. Sci. Technol.* A **10** 3048
[31] Kitajima T, Takeo Y, Petrovic Z Lj and Makabe T 2000 *Appl. Phys. Lett.* **77** 489
[32] Salabas A and Brinkmann R P 2006 *Japan. J. Appl. Phys.* **45** 5203–6
[33] Mussenbrock T, Ziegler D and Brinkmann R P 2006 *Phys. Plasmas* **13** 083501
[34] Ziegler D, Mussenbrock T and Brinkmann R P 2008 *Plasma Sources Sci. Technol.* **17** 045011
[35] Czarnetzki U, Mussenbrock T and Brinkmann R P 2006 *Phys. Plasmas* **13** 123503
[36] Mussenbrock T and Brinkmann R P 2007 *Plasma Sources Sci. Technol.* **16** 377
[37] Lieberman M A, Lichtenberg A J, Kawamura E, Mussenbrock T and Brinkmann R P 2008 *Phys. Plasmas* **15** 063505
[38] Ziegler D, Mussenbrock T and Brinkmann R P 2009 *Phys. Plasmas* **16** 023503
[39] Mussenbrock T and Brinkmann R P 2006 *Appl. Phys. Lett.* **88** 151503
[40] Mussenbrock T, Brinkmann R P, Lieberman M A, Lichtenberg A J and Kawamura E 2008 *Phys. Rev. Lett.* **101** 085004
[41] Kratzer M, Brinkmann R P, Sabisch W and Schmidt H 2001 *J. Appl. Phys.* **90** 2169
[42] Sabisch W, Kratzer M and Brinkmann R P 2003 *J. Vac. Sci. Technol.* A **21** 1205
[43] Heil B G, Brinkmann R P and Czarnetzki U 2008 *J. Phys. D: Appl. Phys.* **41** 225208
[44] Heil B G, Schulze J, Mussenbrock T, Brinkmann R P and Czarnetzki U 2008 *IEEE Trans. Plasma Sci.* **36** 1404
[45] Schulze J, Donko Z, Heil B G, Luggenhölscher D, Mussenbrock T, Brinkmann R P and Czarnetzki U 2008 *J. Phys. D: Appl. Phys.* **41** 105214
[46] Schulze J, Heil B G, Luggenhölscher D, Brinkmann R P, and Czarnetzki U 2008 *J. Phys. D: Appl. Phys.* **41** 195212
[47] Heil B G, Czarnetzki U, Brinkmann R P and Mussenbrock T 2008 *J. Phys. D: Appl. Phys.* **41** 165202